CRCLEME
Cooperative Research Centre for
Landscape Evolution & Mineral Exploration

AMIRA
Australian Mineral Industries Research Association Limited ACN 004 448 266

OPEN FILE
REPORT
SERIES

MINERALOGICAL AND GEOCHEMICAL ASPECTS OF THE REGOLITH AT THE BRAHMAN Au PROSPECT, CHARTERS TOWERS AREA, N.E. QUEENSLAND

K.M Scott and S.J. Fraser

CRC LEME OPEN FILE REPORT 143

March 2002

(CSIRO Exploration and Mining Report 434R/CRC LEME Report 60R, 1997.
Second impression 2002)

AMIRA
Australian Mineral Industries Research Association Limited ACN 004 448 266

CRCLEME
Cooperative Research Centre for
Landscape Evolution & Mineral Exploration

MINERALOGICAL AND GEOCHEMICAL ASPECTS OF THE REGOLITH AT THE BRAHMAN Au PROSPECT, CHARTERS TOWERS AREA, N.E. QUEENSLAND

K.M. Scott and S.J. Fraser

CRC LEME OPEN FILE REPORT 143

March 2002

(CSIRO Exploration and Mining Report 434R/CRC LEME Report 60R, 1997.
Second impression 2002)

CRC LEME is an unincorporated joint venture between CSIRO-Exploration & Mining, and Land & Water, The Australian National University, Curtin University of Technology, University of Adelaide, University of Canberra, Geoscience Australia, Bureau of Rural Sciences, Primary Industries and Resources SA, NSW Department of Mineral Resources-Geological Survey and Minerals Council of Australia.
Headquarters: CRC LEME c/o CSIRO Exploration and Mining, PO Box 1130, Bentley WA 6102, Australia

CSIRO/CRC LEME/AMIRA PROJECT P417
GEOCHEMICAL EXPLORATION IN REGOLITH-DOMINATED TERRAIN, NORTH QUEENSLAND 1994-1997

In 1994, CSIRO commenced a multi-client research project in regolith geology and geochemistry in North Queensland, supported by 11 mining companies, through the Australian Mineral Industries Research Association Limited (AMIRA). This research project, "Geochemical Exploration in Regolith-Dominated Terrain, North Queensland" had the aim of substantially improving geochemical methods of exploring for base metals and gold deposits under cover or obscured by deep weathering in selected areas within (a) the Mt Isa region and (b) the Charters Towers - North Drummond Basin region.

In July 1995, this project was incorporated into the research programs of CRC LEME, which provided an expanded staffing, not only from CSIRO but also from the Australian Geological Survey Organisation, University of Queensland and the Queensland Department of Minerals and Energy. The project, operated from nodes in Perth, Brisbane, Canberra and Sydney, was led by Dr R.R. Anand. It was commenced on 1st April 1994 and concluded in December 1997. The project involved regional mapping (three areas), district scale mapping (seven areas), local scale mapping (six areas), geochemical dispersion studies (fifteen sites) and geochronological studies (eleven sites). It carried the experience gained from the Yilgarn (see CRC LEME Open File Reports 1-75 and 86-112) across the continent and expanded upon it.

Although the confidentiality period of Project P417 expired in mid 2000, the reports have not been released previously. CRC LEME acknowledges the Australian Mineral Industries Research Association and CSIRO Division of Exploration and Mining for authority to publish these reports. It is intended that publication of the reports will be a substantial additional factor in transferring technology to aid the Australian mineral industry.

This report (CRC LEME Open File Report 143) is a second impression (second printing) of CSIRO, Division of Exploration and Mining Restricted Report 434R, first issued in 1997, which formed part of the CSIRO/AMIRA Project P417.

Copies of this publication can be obtained from:
The Publication Officer, c/- CRC LEME, CSIRO Exploration and Mining, P.O. Box 1130, Bentley, WA 6102, Australia.. Information on other publications in this series may be obtained from the above or from http://leme.anu.edu.au/

Cataloguing-in-Publication:
Scott, K.M.
Mineralogical and geochemical aspects of the regolith at the Brahman Au Prospect, Charters Towers area, N.E. Queensland.
ISBN 0 643 06810 4
1. Regolith - Queensland 2. Geochemistry 3. Landforms - Queensland
I. Fraser, S.J. II. Title
CRC LEME Open File Report 143.
ISSN 1329-4768

Addresses and affiliations of authors

Mr K.M. Scott
Cooperative Research Centre for Landscape Evolution and Mineral Exploration
c/- CSIRO Exploration and Mining
PO Box 136
North Ryde NSW 2113
Australia

Mr S.J. Fraser
Cooperative Research Centre for Landscape Evolution and Mineral Exploration
c/- CSIRO Exploration and Mining
PO Box 883
Kenmore QLD 4069
Australia

PREFACE

The CRCLEME-AMIRA Project "Geochemical exploration in regolith-dominated terrain of North Queensland" (P417) has, as its overall aim, to substantially improve geochemical methods of exploring for base metals and gold deposits under cover or obscured by deep weathering. The research includes geochemical dispersion studies, regolith characterisation, dating of profiles and investigation of regolith evolution.

The problem confronting exploration in the Charters Towers-north Drummond Basin is the presence of a variety of sedimentary cover masking prospective basement lithologies. The Campaspe Formation is widespread in the Charters Towers-Mount Windsor Sub-Province and is generally underlain by weathered volcanics. On the one hand, it has commonly been considered unsuitable as a sample medium because of its exotic origin and exploration strategy has relied on drilling through the Campaspe Formation into bedrock. On the other hand, it has been subjected to post-depositional weathering and diagenesis because of its age, and it is thought that there could be potential for mechanical or chemical dispersion from underlying mineralisation. If surficial sampling could be employed and natural dispersion used, exploration costs could be reduced substantially. This report investigates possible dispersion into the overlying Campaspe Formation at Brahman prospect.

Ferruginous pisoliths are developed at the top of the Campaspe Formation at Brahman and indeed in large areas of the region. There is a dispersion for several hundred metres about the Au lode both in the granitic saprolite and also in the surficial ferruginous pisoliths. Arsenic, Cu and Pb contents are also elevated with the Au in the ferruginous pisoliths forming a halo at least 700 x 500 m above the mineralisation. Thus, systematic sampling of the pisolitic unit could represent an effective way to explore in this area to the north of Charters Towers.

R.R. Anand
Project Leader

I.D.M. Robertson
Deputy Leader

TABLE OF CONTENTS

LIST OF TABLES

LIST OF FIGURES

LIST OF APPENDICES

SUMMARY

The regolith at the Brahman Au prospect, is characterized by the presence of ferruginous pisoliths above mottled transported sandstone (Campaspe Formation) which unconformably overlies residual clay and saprolitic granite. Within the profile, Au is laterally dispersed for up to several hundred metres at the top and bottom of the saprolite as well as in the surficial pisoliths. Arsenic, Cu and Pb contents are also elevated in the ferruginous pisoliths. Zones of lateral dispersion of Au with a zone of depletion beneath the surficial anomaly are similar to those commonly observed in the Yilgarn Craton of Western Australia. However, at Brahman, the Au-enriched pisolitic unit and Au-depleted mottled zone are developed in transported material, i.e. Au has been hydromorphically dispersed into the overlying sediments. Manganese oxides and associated elements (Ce, Co, La and Zn) are well developed in the clay zone of the profile, but are also present in transported material suggesting that they are also dispersed late in the history of regolith development.

Despite their probable development in transported material, the ferruginous pisoliths represent a good sampling medium. Orientation results suggest that low level Au, As, Cu and Pb halos at least 700 x 500 m are present even in five metre composite samples that include a large component of non-ferruginous material. More intense anomalies with better signal-to-noise ratios would be expected with purer pisolitic samples which have not been diluted with depleted material. The development of such extensive hydromorphic dispersion over minor mineralization is encouraging for exploration within the Charters Towers region. Anomalous Th (+U) with the pisoliths suggest that airborne radiometrics may be a useful method to assist in the planning a regional pisolith sampling programme.

1. INTRODUCTION

In the Charters Towers - North Drummond Basin region, extensive areas of Tertiary sediments cover prospective basement lithologies. These Tertiary sediments may belong to either of two sedimentary systems: the older Southern Cross Formation or the younger Campaspe Formation. Whereas most of these Tertiary sediments are fluviatile (Henderson and Nind, 1994), locally derived materials eroded from nearby basement lithologies can be significant (e.g. at Thalanga: Taylor and Humphrey, 1991; Scott, 1997). Compositionally, the two Tertiary formations are relatively similar, although the Southern Cross Formation is generally more clay-rich than the Campaspe Formation. Hydromorphic dispersion from base metal deposits into these cover sequences has been reported by Granier *et al* (1989) and further investigated during this project (e.g. Scott, 1995, 1997).

Recently, the extent of the distribution of ferruginous duricrust and pisoliths within the region has become more obvious (Rivers *et al.*, 1996; Scott *et al.*, 1996; Fraser, 1997). Such ferruginous material is potentially a good geochemical sampling medium in arid terrains (e.g. Carver *et al.*, 1987; Smith *et al.*, 1992, Anand *et al.*, 1993). However, because pisoliths and ferricrete are known to be developed in both the Tertiary Campaspe and Southern Cross Formations which overlie the Palaeozoic bedrock of the area (e.g. at Red Falls, 35 km NW of Charters Towers; Scott *et al.*, 1996), their relationship to the underlying saprolite needs to be properly evaluated in this area. The intersection of possible Charters Towers-style Au mineralization beneath a partially buried pisolitic unit at Brahman (35 km west of Charters Towers) thus provides an ideal study area for investigating the geochemistry and mineralogy of regolith materials above Au mineralization in the region. In particular, this study has investigated whether (a) trace elements associated with Au mineralization are dispersed into Tertiary cover sequences; (b) any mineralogical or chemical features which can be related to mineralization/alteration can be seen in the cover; and (c) mineralogical and/or geochemical features can assist in distinguishing the Tertiary sediments from weathered granitic basement.

2. GEOLOGY

Basement geology in the Brahman prospect area is characterized by the occurrence of magnetite-bearing and non-magnetic granites intruding biotite schists of the Charters Towers Metamorphics. Mesothermal mineralization of the Charters Towers vein-style occurs near the boundary of the magnetic granite and the intruded schists. At Charters Towers, such mineralization is characterized by the occurrence of Au in quartz veins with some associated pyrite, galena and sphalerite (Clarke and Paine, 1970). At Brahman (AMG 397194E 777861N), an intersection of 1.5 g/t Au over 4 m has been recorded in one drill hole. The shallow Powthalanga Au workings occur in granite about 1.5 km north west of Brahman (Figure 1). However, at both Brahman and Powthalanga, associated base metal contents appear to be low.

The Brahman area consists of 1-2 m of recent alluvium overlying ferruginous pisoliths, which are generally only exposed in shallow erosion gullies. Drilling indicates that the pisolitic unit may be up to 2 m thick. Below the pisolitic unit, a zone of silicified and ferruginous sandstone often with coarse quartz lenses occurs. Its thickness varies between 5 and 20 m, with its components considered to be derived from granitoids in the region (M. van Eck, 1997, pers. comm), i.e. it is mottled transported material of the Campaspe Formation. Beneath these transported units, 5 to 10 m of residual sandy and puggy clay occurs above ~30 m of saprolitic granite before relatively fresh magnetic granite is encountered at about 50 m depth. A cross section is shown in Figure 2.

Gold > 2 ppb occurs as a horizontal blanket at approximately 15-20 m within the saprolite and into the overlying clay zone (M. van Eck, 1997, pers. comm.). Mineralization below that level is restricted

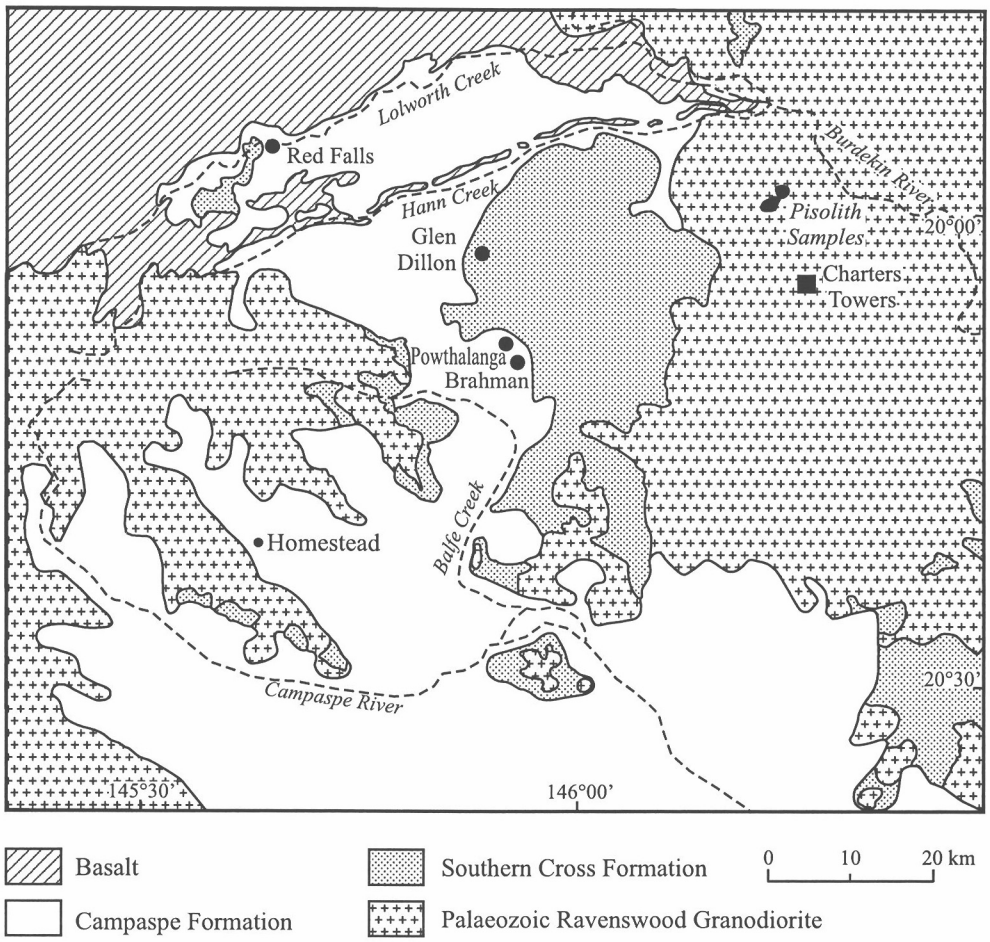

Figure 1 Distribution of Cainozoic units and Brahman Prospect, Charters Towers area *(after Henderson and Nind, 1994).*

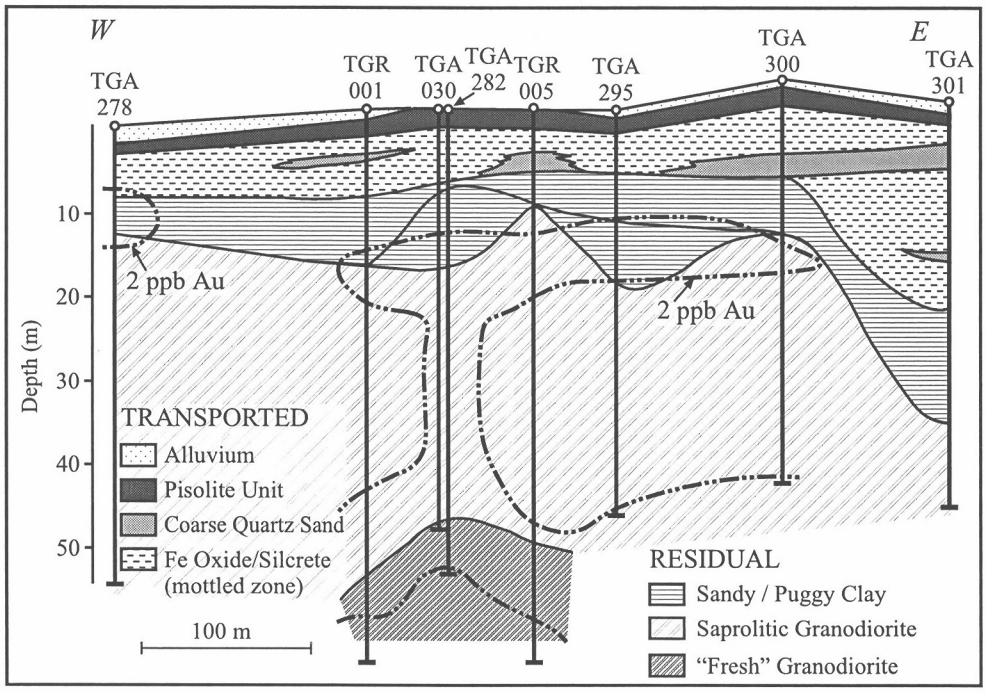

Figure 2 Section through regolith at Brahman - Line 7778800N *(after Marcel van Eck, 1997).*

to a narrow zone about drill holes TGA 030 and 282 until below 40 m where another sub-horizontal enrichment zone is encountered at the base of the saprolite. Despite being only 40m apart, the good grade (1.5 g/t Au) in TGA 030 was not reproduced in TGA 282 or other nearby drill holes.

3. SAMPLES AND METHODS

3.1 Samples

After reviewing the geological and geochemical information for the area (available from Mt Leyshon Gold Mines Ltd), sampling of drill holes from N-S and E-W sections across the Brahman mineralization was considered appropriate. Thus for this pilot study, a total of 151 one metre composite samples from eight air core drill holes (TGA 278, 282, 283, 285, 295, 300, 306, 364) were collected to provide sections across the Brahman mineralization (Figure 3). Samples were collected at metre intervals to 5 m and then every 2 metres to about 30 m, except in TGA 282, the most highly mineralized hole available, for which sampling at a 2 m interval extended to 60 m.

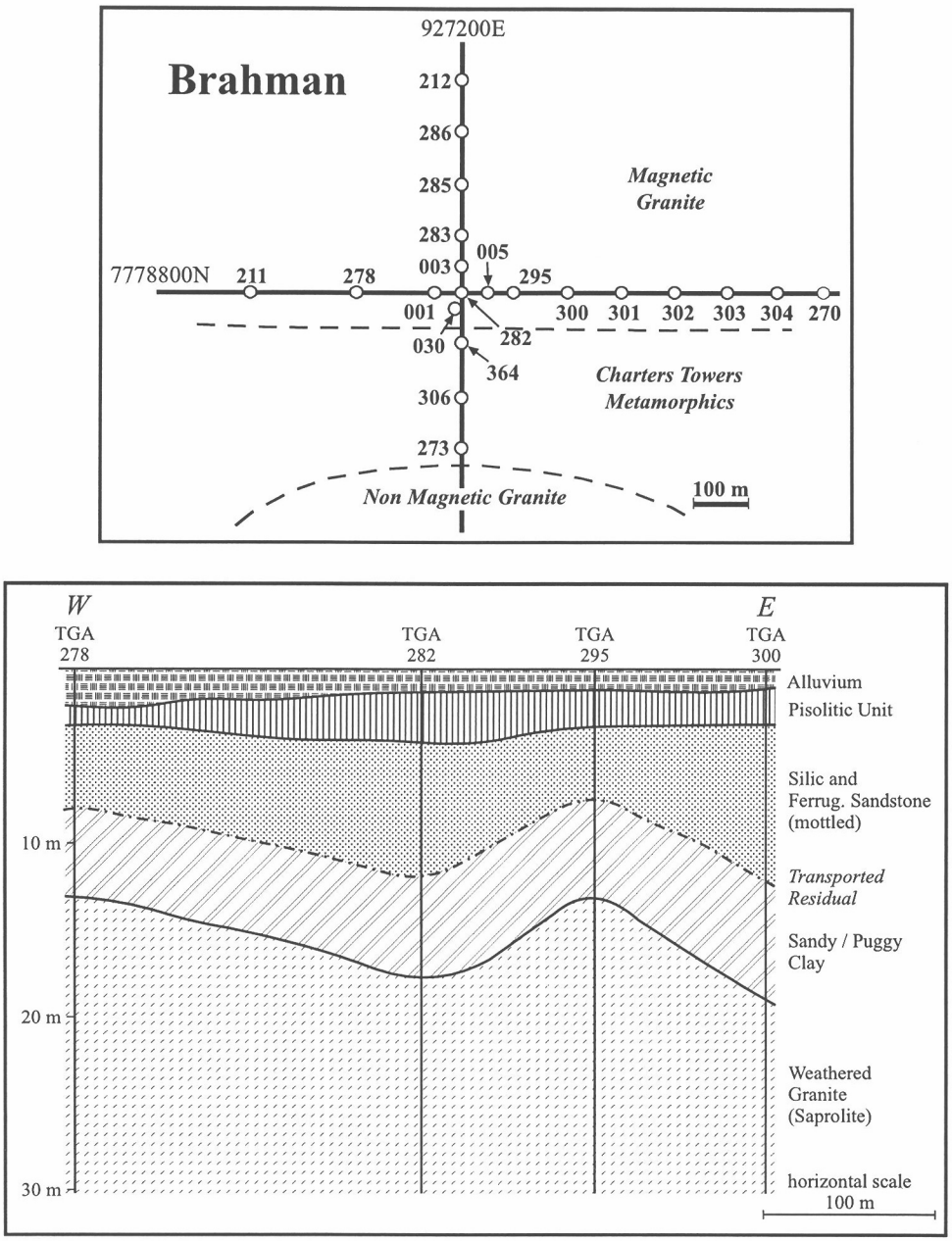

Figure 3 Plan of drill holes and W-E section (77788000N), Brahman.

3.2 Methods

Using all the available geological information and the bulk (5 m) geochemical data supplied by Mt Leyshon Mines Ltd, a group of 50 one - metre composite samples (from drill holes TGA 278, 282, 295 and 300) was crushed to - 75 μm using a Mn-steel mill. These samples were analysed for the "Au + 28 package" by Neutron Activation Analysis (NAA) with Cu, Pb, Zn and Mn being determined by Atomic Absorption Spectrometry after an aqua regia digest. By using extended counting times, the detection limits of most NAA-determined elements has been reduced by a factor of ~2. Thus detection limits during this study were 0.5 ppm As, 2 ppb Au, 50 ppm Ba, 0.5 ppm Br, 2 ppm Ce, 0.5 ppm Co, 2 ppm Cr, 0.5 ppm Cs, 0.5 ppm La, 10 ppm Rb, 0.1 ppm Sb, 0.1 ppm Sc, 0.2 ppm Th, 1 ppm W, 1 ppm U, 0.02% Fe, 0.1% K and 0.01% Na (H. Waldron, 1997, pers. comm.). Abundances of Ag (2 ppm), Ir (5 ppm) Mo (5 ppm) and Se (2 ppm) were below the detection limits indicated in parentheses.

Note that the 5 m composite sampling conducted by Mt Leyshon Gold Mines Ltd used Inductively Coupled Atomic Emission Spectrometry after an aqua regia digest for Fe, Mn, As, Cu, Pb, Zn, with Au being determined down to 0.1 ppb by Atomic Absorption Spectrometry after cyanide leach and solvent extraction.

Samples were analysed spectrally using PIMA II to generate "stacked profiles" of infra-red reflectance spectra over the interval 1300 to 2500 nm. By using this spectral range, one can determine the properties of a number of phyllosilicates (for more detail see Fraser and Scott, 1997) Selected samples from drill holes TGA 278, 282, 283 and 300 along the W-E section were also analysed by X-ray diffractometry (XRD) to determine non-phyllosilicate mineral features.

4. RESULTS

4.1 Mineralogy of the regolith

PIMA II studies of holes from along the W-E and N-S sections reveal a consistent vertical sequence from disordered kaolinite (long wavelength position of the 2160-2180 nm reflectance minimum) → ordered kaolinitie (short wavelength) → Fe-rich smectite → montmorillonite (Fraser and Scott, 1997; Appendix I). Chlorite is generally observed in the deepest samples of each hole, although its upper limit is often difficult to define (Appendix I). K_1, the disordered long wavelength kaolinite, occurs mostly within the transported material whereas K_2, the ordered shorter wavelength kaolinite occurs within the residual material, except for TGA 282 (Figure 4). The presence of a 2239 nm feature in all the kaolinitic samples indicates both types of kaolinite include Fe within their structure. Montmorillonite is restricted to the residual material, with anFe-rich smectite (characterized by a 2295 nm feature) occurring for up to 5 m above the Fe-poor smectite (Figure 5). Although the smectites generally give way to kaolinite in the upper parts of the profile there is strong development of K_2 (ordered kaolinite) in the basal portion of TGA 278.

PIMA II results along the N-S section through TGA 282 suggest that the unconformity may be indicated by the lower limit of K_1 (disordered kaolinite) over metamorphic (schist) bedrock and that kaolinite K_2) is developed to greater depth over such schistose rocks (Figure 6). Smectites (both mont-morillonite and Fe-rich smectite) are only poorly developed over the schistose bedrocks (Figure 7).

XRD profiles for TGA 278 and 282 reveal that plagioclase is present in the weathered profiles up to the base of the pisolitic unit in TGA 278, whereas plagioclase *and* orthoclase are present through that portion of the profile in TGA 282 (Figure 8 and 9). As indicated by the PIMA II studies, kaolinite gives way to smectites at depth, except in TGA 278 where it occurs with chlorite ± calcite below 18m in TGA 278. Chlorite and calcite occur below 41 m in TGA 282 with calcite alone in the transported material to depth of 5 m in TGA 282. Amphibole (hornblende) is present in the deepest

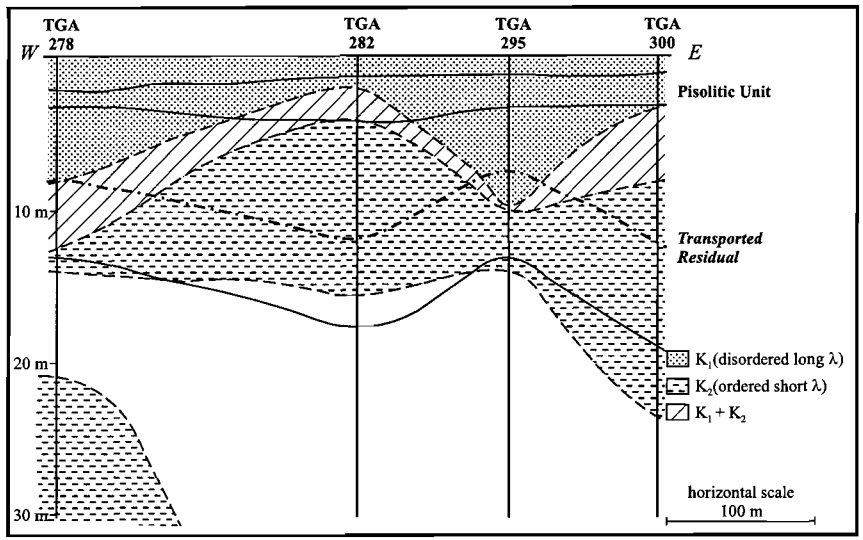

Figure 4 Distribution of kaolinite, W-E Section (77788800N), Brahman.

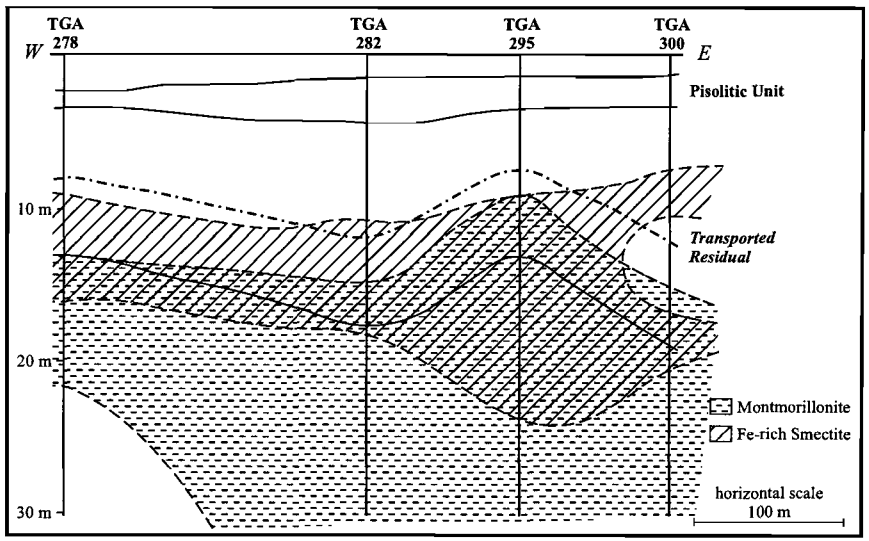

Figure 5 Distribution of smectites, W-E Section (77788800N), Brahman.

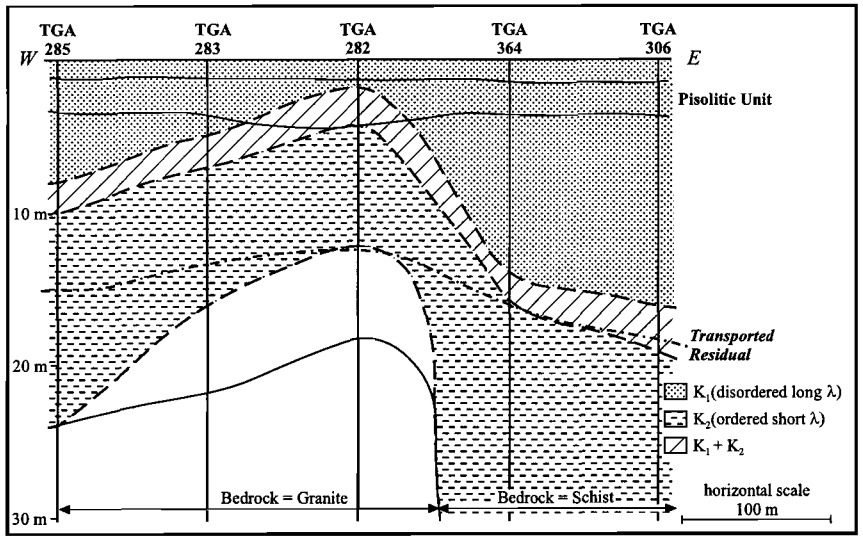

Figure 6 Distribution of kaolinite, N-S Section (397200E), Brahman.

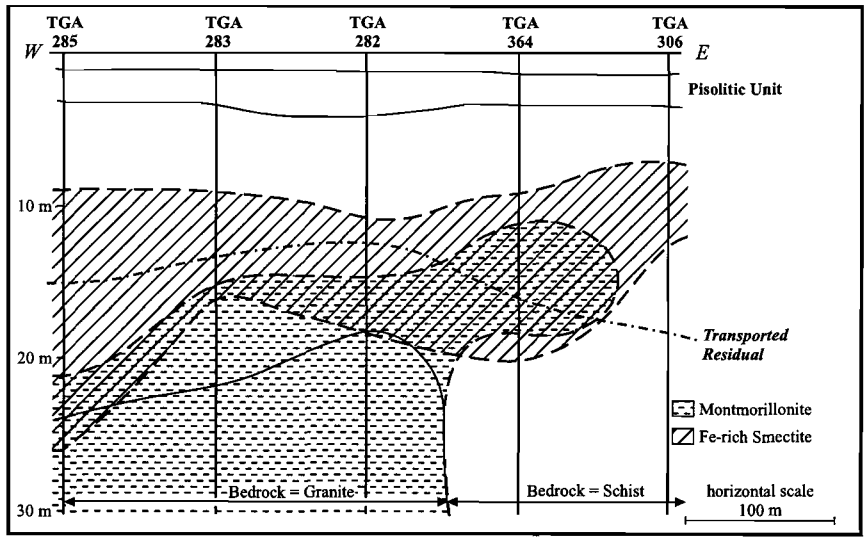

Figure 7 Distribution of smectites, N-S Section (397200E), Brahman.

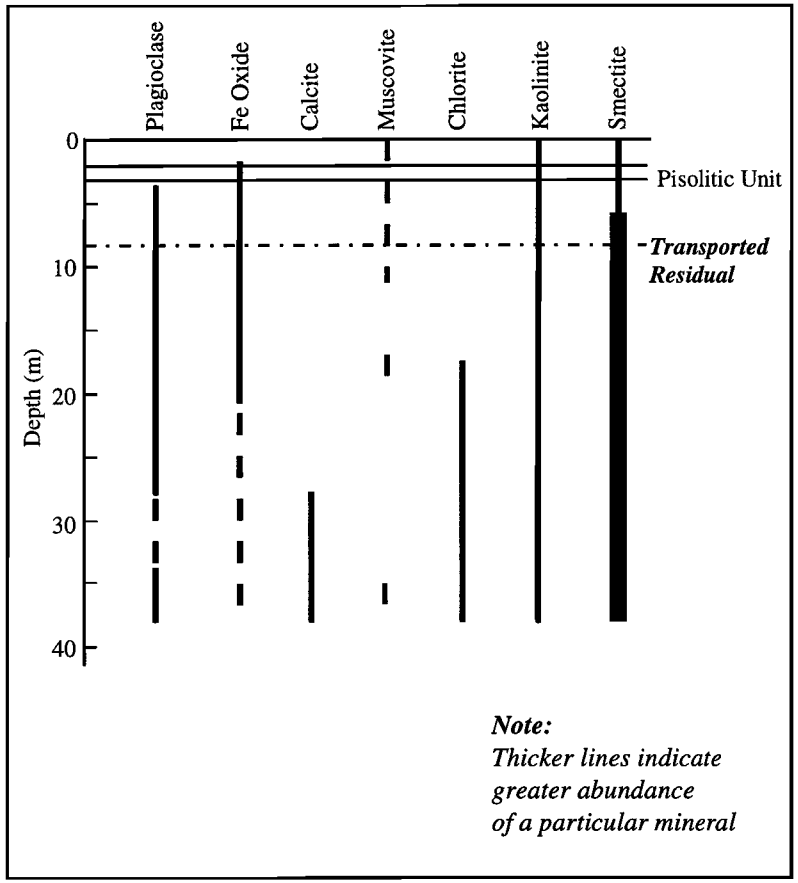

Figure 8 Mineralogy in drill hole TGA 278, Brahman
(determined by X-ray diffraction).

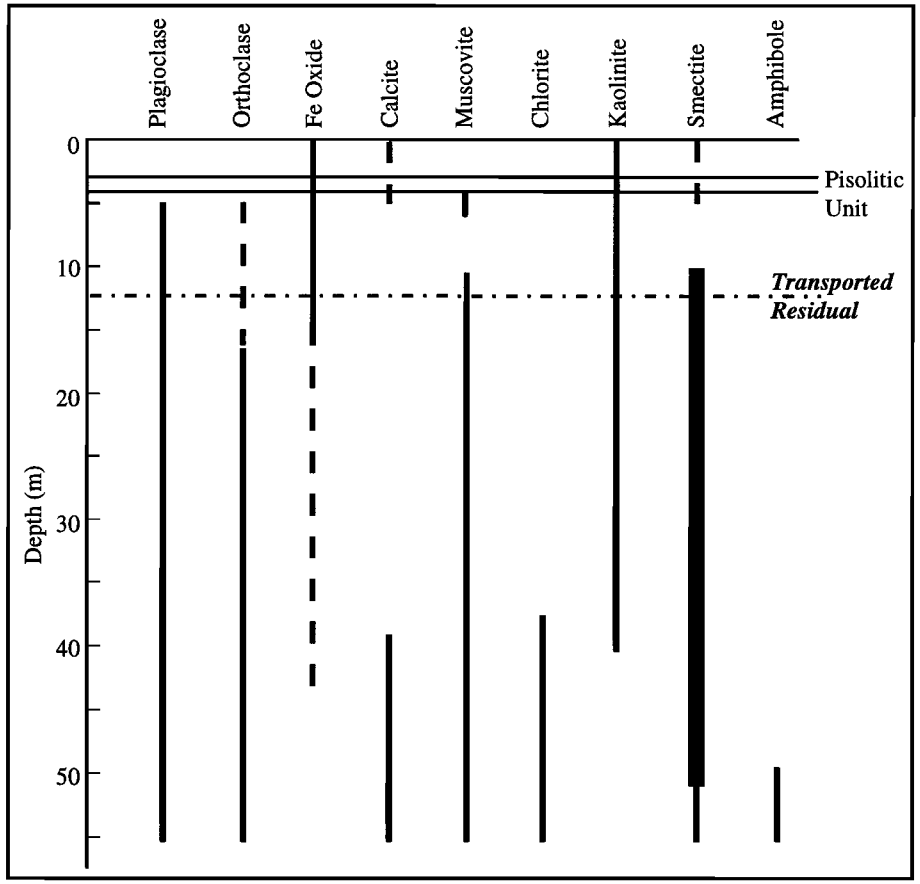

Figure 9 Mineralogy in drill hole TGA 282, Brahman
(determined by X-ray diffraction).

samples from TGA 282. Although muscovite is only intermittently present in TGA 278 it is consistently present as a significant component below 19 m in TGA 282 (Figures 8 and 9).

4.2 Geochemistry of regolith profiles

4.2.1 Drill holes

Analysis of the top 15 m of TGA 278 show that the alluvial horizon is low in Fe and most other components, although it does bear 3.1 ppb Au (Table 1). The pisolitic unit has the highest Fe, As, Cr, Cu, Pb, Rb, Sb, Sc, Th and U contents with the mottled material showing an association between Mn and Ce, Co, La and Zn (Table 1, Appendix II). The residual clay and underlying saprolite may also show the association of these elements with Mn but they also have elevated Au contents (23 ppb). Sodium contents gradually increase down the profile with significant Na in the basal two zones reflecting the presence of plagioclase. Potassium contents are low throughout the profile i.e. in both transported and residual material.

Table 1: Average composition of zones within drill hole TGA278, Brahman Prospect (ppm, unless otherwise indicated)

	Transported Overburden			Residual Profile	
Zone	Alluvial	Pisolitic	Mottled	Clay	Saprolite
Depth (m)	0-2	2-3	3-8	9-12	13-15
Fe%	1.43	18.1	5.80	5.96	7.05
Mn	110	160	(730)	(820)	(1700)
Na%	0.04	0.04	0.11	0.27	0.43
K%	0.17	0.14	0.15	<0.10	0.15
As	2	31	7	2	1
Au(ppb)	3.1	<2	<2	23	3.7
Ba	70	78	300	(180)	430
Br	2	<1	<1	2	<1
Ce	25	40	(120)	32	22
Co	6	26	(53)	27	35
Cr	39	180	53	50	69
Cs	2	3	2	2	1
Cu	18	64	39	51	56
La	11	17	(30)	52	15
Pb	11	46	22	6	<5
Rb	22	34	19	18	27
Sb	0.2	0.9	0.3	0.2	<0.1
Sc	8	26	16	24	24
Th	6	17	10	6	2
W	4	<1	1	<1	<1
U	<1	6	1	<1	<1
Zn	24	26	(47)	62	62

Note: Averages in parentheses include one anomalously high value

In TGA 282, the pisolitic unit again has the highest Fe, As, Cr, Pb, Sb, Th and U contents (Table 2, Appendix III). Although the alluvial unit in this location has higher Au (6.3 ppb) and chalcophile element contents than at TGA 278 (Tables 1 and 2), visual examination indicates that the higher Fe content (5.49% vs 1.43% in TGA 278) reflects the presence of some pisolitic material within the top metre composite. The residual clay and saprolite have some high (>800 ppm) Mn contents with associated Ba, Co, Ce, La and Zn. Gold is anomalous in the top metre (6.3 ppb) and again below 13 m, in the residual material (> 4 ppb, Table 2). Potassium contents are particularly high in the saprolite (K=1.16%) where muscovite and orthoclase are well developed (Table 2, Figure 9). However, K is elevated (> 0.2%) in the transported material at this site relative to TGA 278.

Table 2: Average composition of zones within drill hole TGA282, Brahman Prospect (ppm, unless otherwise indicated)

	Transported Overburden			Residual Profile	
Zone	Alluvial	Pisolitic	Mottled	Clay	Saprolite
Depth (m)	0-1	1-4	4-12	13-16	19-30
Fe%	5.48	11.0	5.23	8.01	5.62
Mn	180	140	(290)	(1600)	870
Na%	0.05	0.07	0.14	0.48	0.45
K%	0.14	0.20	0.31	0.25	1.16
As	7	13	4	3	2
Au(ppb)	6.3	<2	<2	4.1	6.6
Ba	57	200	720	940	660
Br	3	1	2	1	<1
Ce	32	28	23	60	78
Co	15	(12)	(13)	(31)	20
Cr	85	93	47	47	26
Cs	4	3	3	1	2
Cu	34	41	31	38	65
La	11	12	17	34	40
Pb	18	29	15	9	10
Rb	34	32	42	25	63
Sb	0.4	0.4	0.2	0.2	<0.1
Sc	16	19	18	20	27
Th	10	15	10	5	6
W	3	1	2	3	<1
U	3	(3)	1	1	<1
Zn	26	33	44	57	89

Note: Averages in parentheses include one anomalously high value

Alluvial material from TGA 295 has low levels of Fe (< 0.5%) and most analysed trace elements (Table 3) reflecting its sandy composition. The pisolitic unit has the highest Fe, As, Ce, Cr, Pb, Rb, Sb, Th and U, with Mn again showing an association with Ba, Ce, Co, La, Zn especially in the residual clay and saprolite (Table 3, Appendix IV). Gold is elevated in the pisolitic unit (2.9 ppb) and within the residual units (> 3 ppb), with quite anomalous values being recorded in the saprolite (Table 3). Although K decreases from a high of 0.7% in the saprolite, K > 0.2% is present through the whole profile below the alluvium. Sodium also shows this marked decrease as the alluvium is encountered (Table 3).

Table 3: Average composition of zones within drill hole TGA295, Brahman Prospect (ppm unless otherwise indicated)

	Transported Overburden			Residual Profile	
Unit	Alluvial	Pisolitic	Mottled	Clay	Saprolite
Depth (m)	0-1	1-3	3-8	9-14	15-20
Fe%	0.46	7.28	4.51	410	3.80
Mn	100	230	130	(2100)	(1200)
Na%	0.01	0.16	0.15	0.18	0.70
K%	<0.10	0.34	0.38	(0.22)	(0.71)
As	1	8	3	1	1
Au(ppb)	<2	2.9	<2	3.0	24
Ba	<50	140	(890)	(690)	650
Br	1	2	2	<1	<1
Ce	16	89	19	72	38
Co	5	19	10	47	21
Cr	24	79	42	32	21
Cs	1	4	3	2	2
Cu	8	39	27	37	34
La	9	17	15	31	30
Pb	6	25	11	11	10
Rb	13	42	41	34	42
Sb	0.1	0.4	0.2	0.1	<0.1
Sc	3	18	17	18	20
Th	4	12	9	8	6
W	1	1	1	2	2
U	<1	3	<1	1	<1
Zn	9	33	46	61	56

Note: Averages in parentheses include one anomalously high value

Within the TGA 300 profile, the pisolitic unit is enriched in Fe,Mn, As, Co, Ce, Cr, Cu, Pb, Sb, Sc, Th and U reflecting the presence of some Mn enrichment in the Fe-rich zone (Table 4, Appendix V). Manganese and associated Co, La and Zn are also developed in the lower portion of the transported unit and the underlying residual clay zone (Table 4). Gold is present in the lower part of the transported material (specifically in the sandy unit) where Au = 3.5 ppb and in the underlying residual material (> 2 ppb). Potassium and Na are present in significant amounts (> 0.2% and > 0.1% respectively) below the alluvial material throughout the profile (Table 4) i.e. in both transported and residual material.

Table 4: Average composition of zones within drill hole TGA300, Brahman Prospect (ppm unless otherwise indicated)

		Transported Overburden			Residual Profile	
Unit	Alluvial	Pisolitic	Mottled	"Sandy"	Clay	Saprolite
Depth (m)	0-1	1-3	3-8	9-12	13-18	19-20
Fe%	0.76	14.5	5.91	3.19	4.64	4.66
Mn	240	1200	240	1100	(1700)	400
Na%	0.02	0.10	0.13	0.16	0.12	0.65
K%	0.16	0.28	0.48	0.71	0.35	1.34
As	1	18	5	1	2	1
Au(ppb)	<2	<2	<2	3.5	2.2	5.2
Ba	72	(350)	(450)	550	730	830
Br	2	1	1	2	<1	<1
Ce	21	(170)	20	75	58	60
Co	5	24	10	19	(28)	14
Cr	26	130	42	30	38	25
Cs	1	3	4	3	2	4
Cu	13	57	35	26	35	38
La	10	19	14	30	39	32
Pb	5	(48)	18	16	14	12
Rb	17	37	58	71	29	52
Sb	0.1	0.8	0.3	0.1	0.2	<0.1
Sc	5	23	19	11	23	23
Th	6	16	11	8	11	7
W	2	<1	1	1	2	2
U	1	4	<1	1	1	<1
Zn	18	37	52	54	76	68

Note: Averages in parentheses include one anomalously high value

4.2.2 Elemental variations in the regolith

The strong association of Fe with chalcophile elements in the pisolitic unit (seen above) is readily observed when the distributions of Fe, As, Cu and Pb are plotted (Figures 10-13). Iron is also seen to be concentrated at the top of the residuum (Figure 10). Gold >2 ppb occurs within both the alluvium and top of the pisolitic unit in holes TGA 278-295 *and* in the clay-rich residuum i.e. Au is concentrated at the top of both the transported and residual portions of the profile (Figure 14). Elevated Au is also seen deeper in TGA 282. Higher K contents are associated with both the residual and transported material in the more easterly portion of the section (Figure 15).

5. DISCUSSION

5.1 Regolith development

The regolith at Brahman is characterized by the presence of pisoliths above mottled transported sandstone (Campaspe Formation) which unconformably overlies residual clay and saprolitic granite. Because PIMA measurements reflect vibrations of molecular bonds and hence features of stacking within molecular units rather than long distance crystallographic order (as does XRD), the combination of the two techniques gives very detailed information about the minerals present in the profiles at Brahman. In particular, the XRD results suggest that the granite weathers firstly by the destruction of amphibole, chlorite and calcite (and some feldspar) to form montmorillonite which in turn weathers to kaolinite (e.g. Figure 9). PIMA indicates that kaolinite formed by weathering of residual material tends to be well ordered (K_2 e.g. Figure 4). Kaolinite is also present in the transported material above the unconformity but such kaolinite tends to be disordered (K_1). There is generally a zone of overlap between the two kaolinite types with the base of the disordered kaolinite (K_1) showing good agreement with the mapped unconformity above schist (Charters Towers Metamorphics) to the south of TGA 282 (Figure 6) but not above granite (Figure 4).

Within the residual material (clay and saprolite), well ordered kaolinite occurs above schistose bedrock, whereas montmorillonite is more abundant above the granite (Figures 6 and 7). This difference is readily identified in PIMA spectra, so that PIMA II could offer an useful way for rapidly determining bedrock type in the area.

Differences in the degree of ordering of kaolinite have sometimes been used to differentiate between residual (ordered kaolinite) and transported materials (disordered kaolinite) using PIMA (Pontual and Merry, 1996). However, as indicated above, at Brahman there is often poor correspondence between the unconformity and the change in kaolinite ordering, especially in hole TGA 282). If the logging accurately reflects the unconformity (see below), the presence of ordered kaolinite (K_2) in transported material may reflect kaolinite formed *in situ* by the same processes/similar fluids as affected residual material, perhaps by weathering of feldspars within the Campaspe Formation after its deposition. Development of well-ordered kaolinite in the Campaspe Formation could reflect acid weathering (acidity being derived from weathering sulfides) and the possibility of sulfide associated mineralisation at depth. Thus the extent of the development of well-ordered kaolinite in the Campaspe Formation should be studied further.

The origin of the vertically extensive zone of well ordered kaolinite (K_2) below 23 m in TGA 278 (Figure 4, Appendix I) is unclear. However its presence, adjacent to Charters Towers lode-style alteration which has associated K enrichment (orthoclase and muscovite) could suggest that the kaolinite reflects either alteration of a readily weathered hydrothermal component or even original argillic alteration. Further work to determine the extent of such kaolinite development in granitic saprolite is thus warranted.

The distribution of the Fe-rich smectite above the montmorillonite and about the logged unconformity is consistent with a "lateritic-type" profile starting to develop prior to the deposition of the Campaspe Formation cf. similar Fe enrichment found at the top of residuum at Waterloo (Scott, 1995). Under this scenario, granite would weather to saprolite and clay-rich material with some Fe starting to be concentrated on the surface, possibly even forming a moderately ferruginous crust. But if such a crust did form, it has been stripped away prior to deposition of the Campaspe Formation sediments. Nevertheless, the presence of Fe-rich smectite reflects an Fe-enriched palaeosurface. However the poor development of kaolinite suggests such a profile, prior to deposition of the Campaspe Formation, was immature. After deposition of the Campaspe Formation weathering has affected both the cover and residual sequence with new lateritic profile (including development of pisoliths within the

Campaspe Formation) superimposed upon the previously weathered materials to produce the profile seen today.

5.2 Geochemistry

Three distinctive elemental associations are present in the regolith - an Fe association, an Au association and an Mn association. The association between Fe and chalcophile elements (As, Cr, Cu, Pb, Sb, Sc, Th and U) is strongly developed in the ferruginous pisolitic unit (Tables 1-4; Figures 10-13). It is also noteworthy that Au tends to occur in the upper part of the pisolitic unit and even

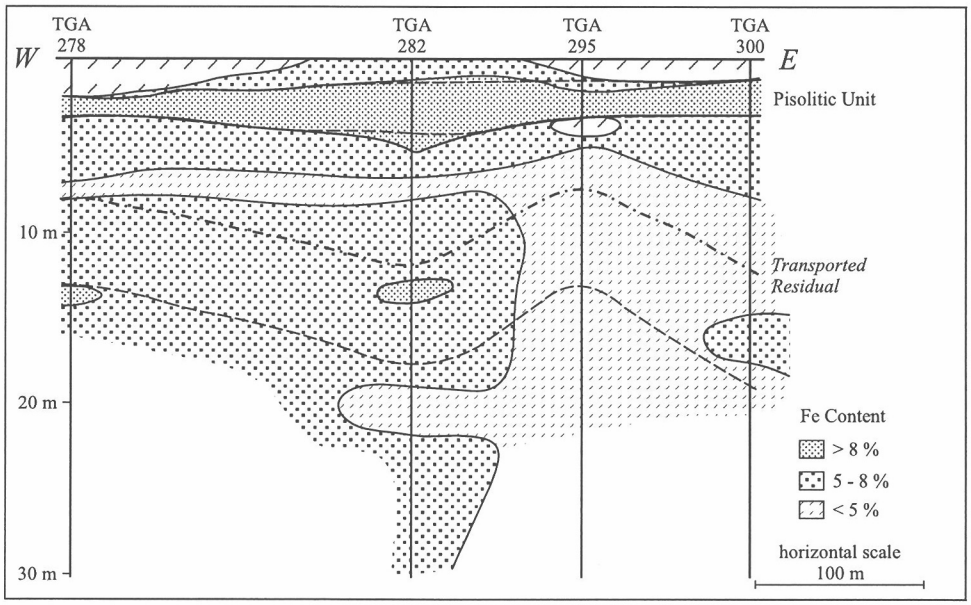

Figure 10 Distribution of Fe, W-E Section (7778800N), Brahman.

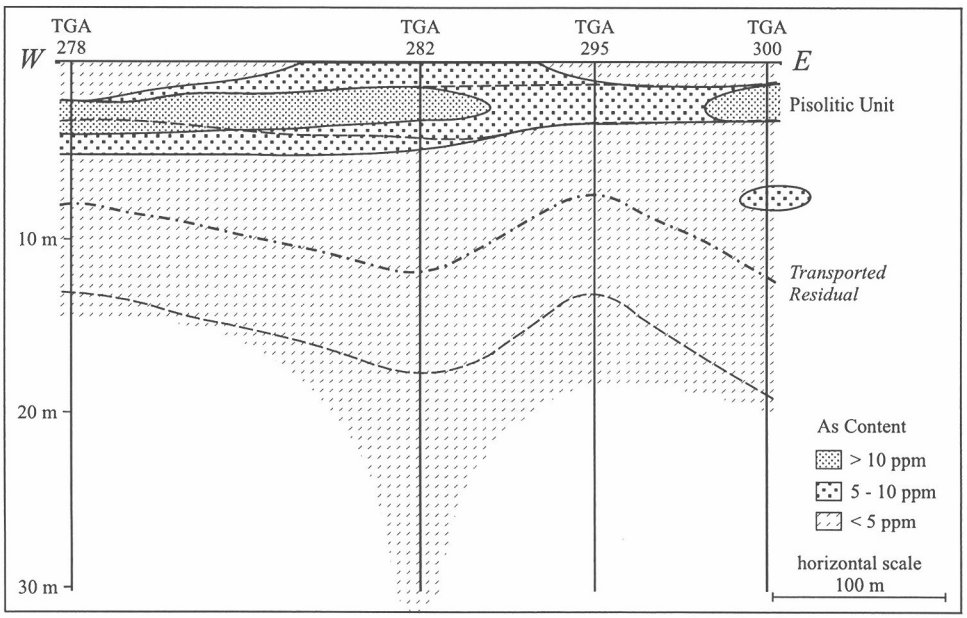

Figure 11 Distribution of As, W-E Section (7778800N), Brahman.

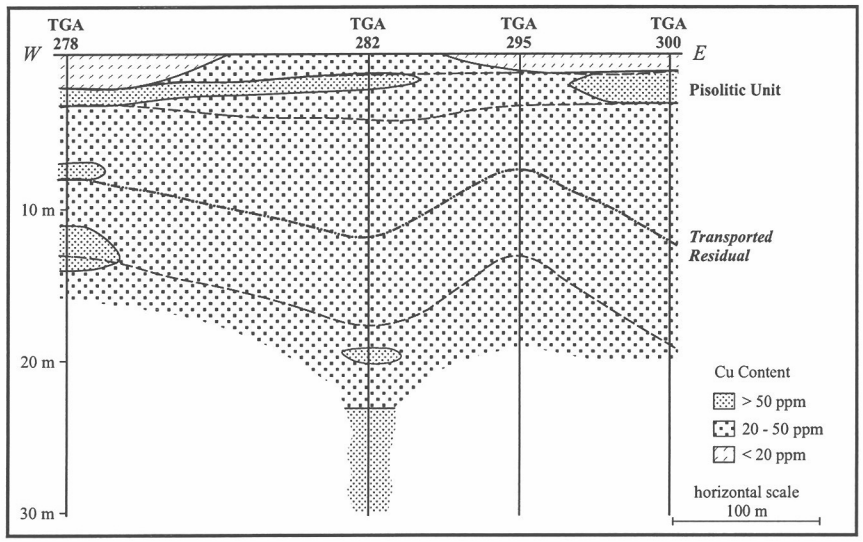

Figure 12 Distribution of Cu, W-E Section (7778800N), Brahman.

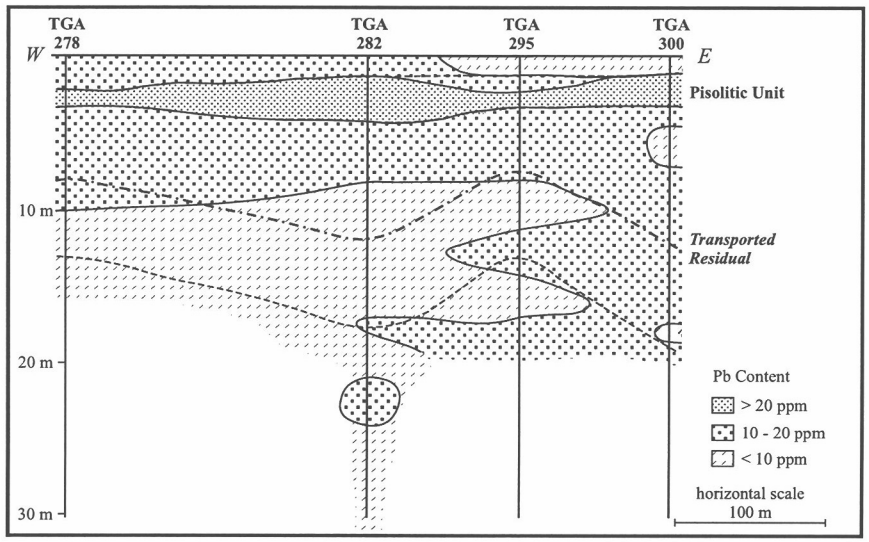

Figure 13 Distribution of Pb, W-E Section (7778800N), Brahman.

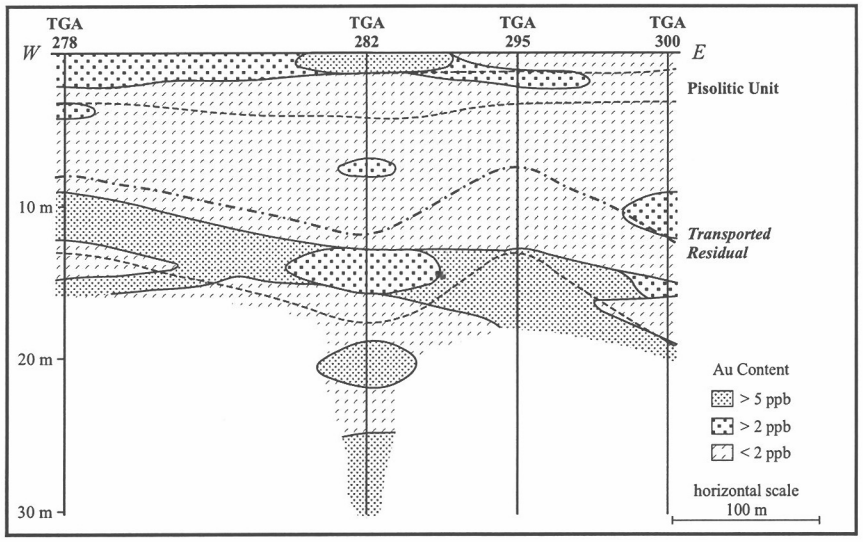

Figure 14 Distribution of Au, W-E Section (777800N), Brahman.

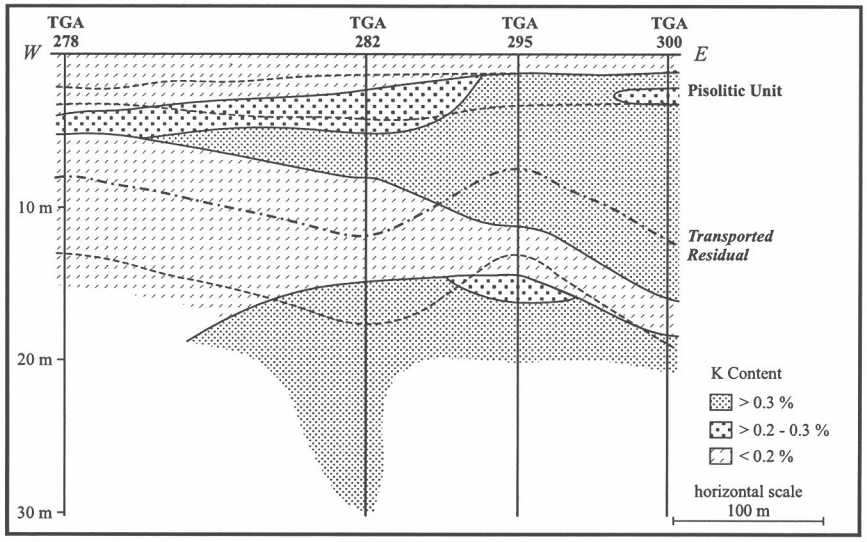

Figure 15 Distribution of K, W-E Section (7778800N), Brahman.

into the alluvial material (Figure 14). This latter feature reflects the presence of some pisolitic/ferruginous material in the composite sample, as seen by the accompanying elevated Fe and associated elements in such samples (see below). Below the pisolitic unit, Au is not present in the transported material but is present in the residual clay and saprolite for several hundred metres about TGA 282 at 10-15 m and probably for similar distances at the base of the saprolite (Figure 3). Such a distribution is similar to that found in the Yilgarn Craton of Western Australia where anomalous Au is found in the ferruginous lateritic residuum and at several horizons within the saprolite (including at its base) with a zone of depletion between the lateritic material and upper saprolitic enrichment zone (Butt, 1988). However at Brahman, abundances are 2-3 orders of magnitude less than in the Yilgarn Craton and all the material above the upper saprolitic enrichment zone is considered transported rather than residual. Thus at Brahman, the presence of Au in the sandy unit within the Campaspe Formation implies that Au has been hydromorphically dispersed into the Tertiary cover.

The Mn-associated elements (Ce, Co, La, Zn and sometimes Ba), although best developed in the clay zone at the top of the residual profile, may be present in the units above and below that interval, even including the pisolitic unit. The presence of the Mn association into the mottled Campaspe material suggests that the development of the Mn oxides is a late phenomenon.

As indicated in Sections 4.2 and 4.3, K is consistently lower in drill hole TGA 278 than in the other holes (Figure 15). Although it is possible that the Campaspe Formation in TGA 278 has a different (low K) source than locations further to the east, the presence of low K material in residuum below may suggest that the origin of the residual and transported low-K material is linked. Thus it can be postulated that either post-Campaspe Formation weathering has strongly leached K in this location or that the whole profile below the alluvium is in fact residual. If this latter alternative is so, the distribution of Au would be quite analogous to distributions in the Yilgarn and the change in kaolinite ordering at 5-10 m depth would be purely a weathering feature rather than a reflection of transported/residual origin. Further work to document variations in K and feldspar contents within other profiles should be undertaken to help access the significance of the low K and lack of orthoclase in the TGA 278 profile. Additional analytical work, especially to determine Ti/Zr contents and other potential geochemical discriminants, might also prove useful, although Scott (1997) found that such discriminants were often of limited value when the Campaspe Formation overlies felsic rocks.

6. THE IMPLICATIONS FOR PISOLITH SAMPLING

Because of the probable association of elevated As, Cu and Pb with anomalous Au in the pisolitic unit (Figures 11-14), the potential for using pisolith sampling at Brahman is briefly considered. The success of pisolith sampling in the Yilgarn Craton of Western Australia relies upon focussing upon ferruginous pisoliths and excluding other material (Smith *et al.*, 1992, Anand *et al.*, 1993). However, some guide to the extent of the anomalies in the pisolitic unit at Brahman can be obtained by using company data from 1-6 m in drill holes (i.e. the 5 m composite from immediately below the alluvium). It is recognised that by using such a sample (including both pisolitic and underlying less ferruginous material), the magnitude of anomalies is reduced from those quoted above (when 1 m composites were used). Nevertheless one can deduce that near surficial ferruginous 5 m samples with Au $\geq$ 0.6 ppb form a coherent zone at least 700 x 500 m about the mineralization in TGA 030 (Figure 16). Arsenic > 2 ppm forms a tighter zone 500 x 200 m restricted to the pisoliths above the magnetic granite (Figure 17). Copper > 20 ppm is also restricted to the material overlying the magnetic granite (Figure 18) but is slightly more extensive in a northerly direction than the As anomaly. Lead > 15 ppm forms an anomaly at least 700 x 600 m (Figure 19) only slightly displaced from the Au anomaly (cf. Figure 16). This preliminary assessment suggests that extensive Au and Pb haloes at least

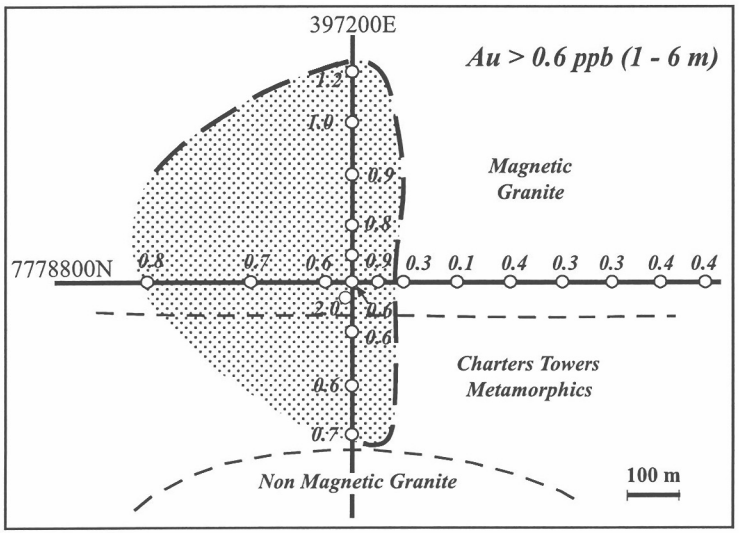

Figure 16 Distribution of Au in 1-6 m samples, Brahman
(data from Mt Leyshon Gold Mines Ltd).

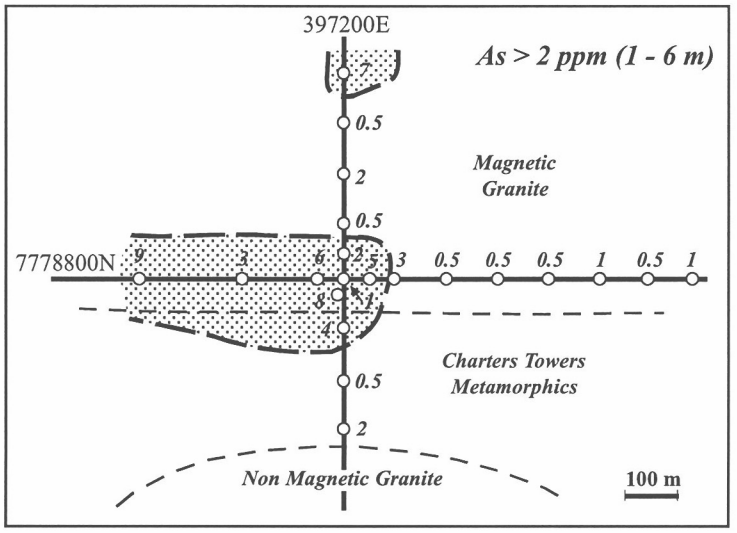

Figure 17 Distribution of As in 1-6 m samples, Brahman
(data from Mt Leyshon Gold Mines Ltd).

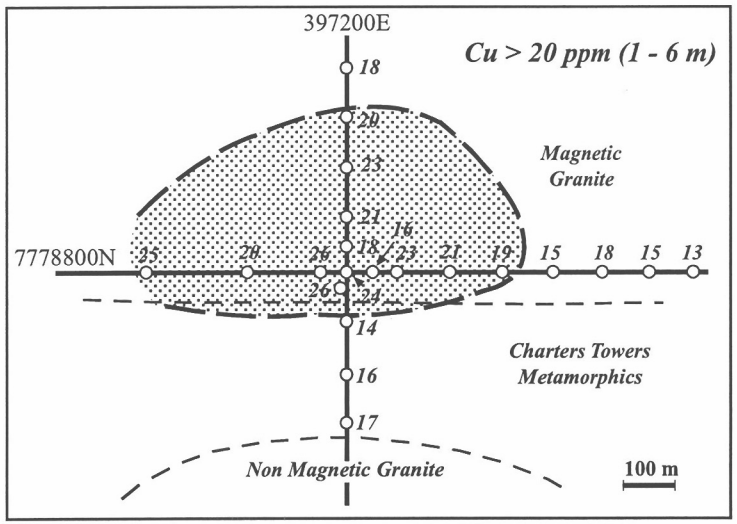

Figure 18 Distribution of Cu in 1-6 m samples, Brahman
(data from Mt Leyshon Gold Mines Ltd).

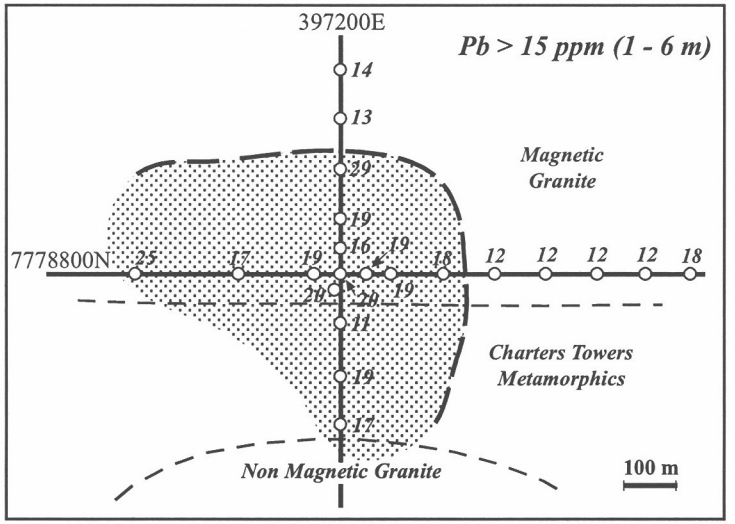

Figure 19 Distribution of Pb in 1-6 m samples, Brahman
(data from Mt Leyshon Gold Mines Ltd).

700 x 500 m occurs in the pisolitic unit above the mineralization at Brahman just below the alluvial cover. Smaller Cu and As haloes also occur. However, the occurrence of 88 ppm As with 3 ppb Au in the pisoliths above barren, non-magnetic granite 800 m SW of the Brahman mineralization (Table 5) suggests that the abundance of As may not by itself necessarily be a good vector to mineralization within broad Au anomalies.

Table 5 Compositions of selected pisolitic samples, Brahman-Charters Towers area (ppm unless otherwise indicated).

Location	Fe %	Au(ppb)	As	Cu	Pb	Zn
Brahman TGA 278 (2-3 m)	18.1	<2	31	64	46	26
Brahman TGA 282 (1-4 m)	11.0	<2	13	41	29	33
0.8 km SW of Brahman	12.6	3	88	56	82	47
1 km W of Brahman	8.7	6	26	130	36	17
11 km NNW of Brahman (Glen Dillon)	16.6	<5*	21	57	65	17
10 km NW of Charters Towers (30 km NE Brahman)	20.4	10	51	81	48	17
11 km NNW of Charters Towers	12.5	<5*	25	82	72	24

*detection limits by standard NAA procedure, lower detection limit needed

The occurrence of Au > 2 ppb, sometimes associated with significant As and base metal contents, within pisoliths from the Charters Towers areas (Table 5) suggests that ferruginous cappings/ferricrete/pisoliths may well be useful sample media in the area. Furthermore, the occurrence of dispersion for hundreds of metres about minor mineralization suggests that hydromorphic dispersion is a very significant factor during weathering and that larger deposits may show even more extensive dispersion haloes. The presence of elevated Th (and U) in the pisolitic samples (Tables 1-4) suggests that areas with potential for pisolith sampling may be identified during radiometric surveys.

7. CONCLUSIONS

This mineralogical and geochemical study shows that Fe and chalcophile elements are strongly associated in a pisolitic unit developed in transported overburden at Brahman and that Mn (and Ce, Co, La, Zn and, sometimes, Ba) are strongly developed in the clay-rich zone at the top of the residual profile. It also suggests that K and orthoclase abundances in the mottled unit developed within transported overburden are strongly influenced by the K and orthoclase content of the underlying residual units. However, kaolinite is noted to change from poorly ordered to well ordered at or near the mapped transported/residual boundary. Thus some doubt about the true nature of the transported material exists.

The vertical and lateral distribution of Au at Brahman is similar to that commonly encountered in the Yilgarn Craton of Western Australia, although abundances are lower by several orders of magnitude at Brahman. In both cases, anomalous Au occurs laterally dispersed in the ferruginous capping to the profile above a zone where Au is depleted. Saprolitic dispersion of Au for several hundred metres about the mineralized zone also occurs in the residual clay zone and at the base of the saprolite. However at Brahman the depleted zone and enriched pisolitic zone appear to be developed in transported overburden. If this is so, it implies that Au has been hydromorphically dispersed. Manganese (and its associated elements) also appears to be hydromorphically dispersed into the transported material.

The profile studies indicate that Au is dispersed for at least 200 m laterally within the profile at Brahman including in the surficial/near surface pisolitic unit. (Arsenic, Cu and Pb are also elevated in this unit about the mineralization). Studies using pisolith-rich samples from about the mineralization suggest that Au and Pb are anomalous for at least 700 x 500 m whereas As and Cu are also anomalous over slightly smaller areas. The development of such extensive haloes about this minor mineralization suggests that hydromorphic dispersion is well developed in the region. Thus systematic sampling of the pisolitic unit could represent an effective way to explore in this area to the north of Charters Towers. Elevated Th (and U) within pisolitic material suggests that airborne radiometric surveys may be useful in planning a regional pisolitic sampling programme.

8. ACKNOWLEDGEMENTS

The support of Mt Leyshon Gold Mines Ltd in conducting the initial sampling and supplying background information for this study is greatly appreciated. In particular, discussions with Tom Orr and Marcel van Eck are gratefully acknowledged. Comments by Ravi Anand and Sylvie Marshall on an earlier draft of the text are also appreciated.

Samples were crushed by Jeff Davis and analysed by XRD by Ken Kinealy. Chemical analyses were performed at Becquerel Laboratories. Diagrams were prepared by Eva Mylka and Jane Michie.

9. REFERENCES

Anand, R.R., Smith, R.E., Phang, C., Wildman, J.E., Robertson, I.D.M. and Munday, T.J.M., 1993. Geochemical exploration in complex lateritic environments of the Yilgarn Craton, Western Australia. CSIRO/AMIRA Project 240A: Yilgarn lateritic environments. CSIRO Division of Exploration Geoscience Restricted Report 442R (297 pp. + appendices).

Butt, C.R.M., 1988. Genesis of supergene gold deposits in the lateritic regolith of the Yilgarn Block, Western Australia in (R.R. Keays, W.R.H. Ramsday and D.I. Groves, Eds) The geology of gold deposits: the perspective in 1988. Economic Geology Monograph 8: 460-470.

Carver, R.N., Chenoweth, L.M., Mazzucchelli, R.H., Oates, C.J. and Robins, T.W., 1987. "Lag" - a geochemical sampling medium for arid regions. Journal of Geochemical Exploration 38: 183-199.

Clarke, D.E. and Paine, A.G.L., 1970. Explanatory notes on the Charters Towers Geological Sheet, Queensland. Bureau of Mineral Resources, Geology and Geophysics (34 pp).

Fraser, S.J., 1997. A Regional Overview of the Charters Towers - North Drummond Basin Region : Geomorphic Landscape Provinces. CRC LEME Restricted Report 39R/CSIRO Exploration and Mining Report 366R (27pp + appendix).

Fraser, S.J and Scott, K. M., 1997. Mineralogy of the regolith at the Brahman Au Prospect, NE Queensland, as determined using PIMA-II Spectroscopy. CSIRO Exploration and Mining Report 440R.

Granier, C., Hartley, J., Michaud, J.C. and Troly, G., 1989. Contribution de la géochimie tridimensionnelle à la découverte, sous couverture allochtone, d'extensions du gisement polymétallique de Thalanga (Queensland, Australie). Journal of Geochemical Exploration 32: 467-475.

Henderson, R.A. and Nind, M.A.P., 1994. Tertiary units, landscape and regolith of the Charters Towers region in New development in geology and metallogeny: Northern Tasman Orogenic Zone (Eds. R.A. Henderson and B.K. Davis) Economic Geology Research Unit, James Cook University of North Queensland., Contribution 50: 17-21.

Pontual, S. and Merry, N., 1996. An exploration strategy to aid the differentiation of residual and transported kaolinites using field-based spectral analysis. AusSpec International Restricted Report SDP003 (112 pp).

Rivers, C.J., Eggleton, T. and Beams, S.D., 1996. Ferricretes and deep weathering profiles of the Puzzler Walls, Charters Towers, north Queensland. AGSO Journal of Australian Geology and Geophysics 16(3): 203-211.

Scott, K.M., 1995. Secondary dispersion about the Waterloo polymetallic deposit, Mt Windsor Sub-province, N.E. Queensland. CSIRO Exploration and Mining Report 168R (30 pp.).

Scott, K.M., 1997. The significance of Campaspe-dominated terrains in exploration within the Mt Windsor sub-province, N.E. Queensland. CRC LEME Restricted Report 58R/CSIRO Exploration and Mining Report 422R (33pp).

Scott, K., Shu, L., Fraser, S., Campbell, I.D., Anand, R.R. and Robertson, I.D.M., 1996. Charters Towers-North Drummond Basin Field Excursion - Field Guide. CRC LEME Restricted Report 11R/CSIRO Exploration and Mining Report 286R (74 pp).

Smith, R.E., Anand, R.R., Churchward, M.M., Robertson, I.D.M., Grunsky, E.G., Grey, D.J., Wildman, J.E. and Perdrix, J.L., 1992. Laterite geochemistry for detecting concealed mineral deposits, Yilgarn Craton, Western Australia. CSIRO/AMIRA Project 240 : Laterite Geochemistry. CSIRO Division of Exploration Geoscience Restricted Report 236R (170 pp).

Taylor, G.F. and Humphrey, C., 1991. An orientation survey of surficial rocks from the Thalanga area, N.E. Queensland. CSIRO Division of Exploration Geoscience Restricted Report 206R. (70p).

APPENDIX I : PIMA II RESULTS

Overall the PIMA spectra are noisy and in retrospect a longer integration interval should have been chosen for their acquisition. Tables A-1 to A-8 summarize the interpretation of the drill hole sample spectra.

The spectra tend to be dominated by the "clay" responses of kaolinite and montmorillonite with some meaningful distribution patterns evident. Two "end-members" of kaolinite spectra were observed over the prospect. A near-surface, (weathering-related ? disordered ?) kaolinite (K1), which has a longer wavelength position in the 2160-2180 nm reflectance minima (i.e., at approx. 2180 nm) occurs in the upper parts of the profile. With increasing depth, there is a transition to a kaolinite (K2) that has a shorter wavelength position in the 2160-2180 nm minima (i.e., at 2160 nm).

An absorption feature at 2239nm appears to be related to Fe substitution within the kaolinites and this feature occurs within both the K1 and K2 varieties.

As a general statement the kaolinitic responses tend to dominate the spectra in those samples collected closer to the surface and there is general transition to smectite-dominated mineral spectra at depth.

Fe-rich smectite (characterized by a reflectance minima at 2295nm) however appears to be restricted to the kaolinite/smectite transition zone.

Table A-1 Salient Spectral Features Drill Hole TGA 278

0 - 8 m	K1 kaolinite
8 - 12 m	mixture of K1 and K2 kaolinite responses
13 - 14 m	mixture of montmorillonite and K2 kaolinite responses
15 - 20 m	strong montmorillonite, possible v weak chlorite(?) response
21 - 22 m	strong montmorillonite, weak K2 kaolinite and v weak chlorite responses
23 - 33 m	strong K2 kaolinite, weak montmorillonite and v weak chlorite responses
33 - 38 m	strong K2 kaolinite, weak montmorillonite and weak chlorite responses

The 2239nm Fe-OH-Al absorption feature, which is considered to be associated with Fe-substitution into kaolinites, appears to be present throughout the hole.
The 2295nm feature, which is considered to be related to the presence of an Fe-rich smectite, is strongly present over the 9 -16m interval.

Stacked Spectral Profile **TGA 278**

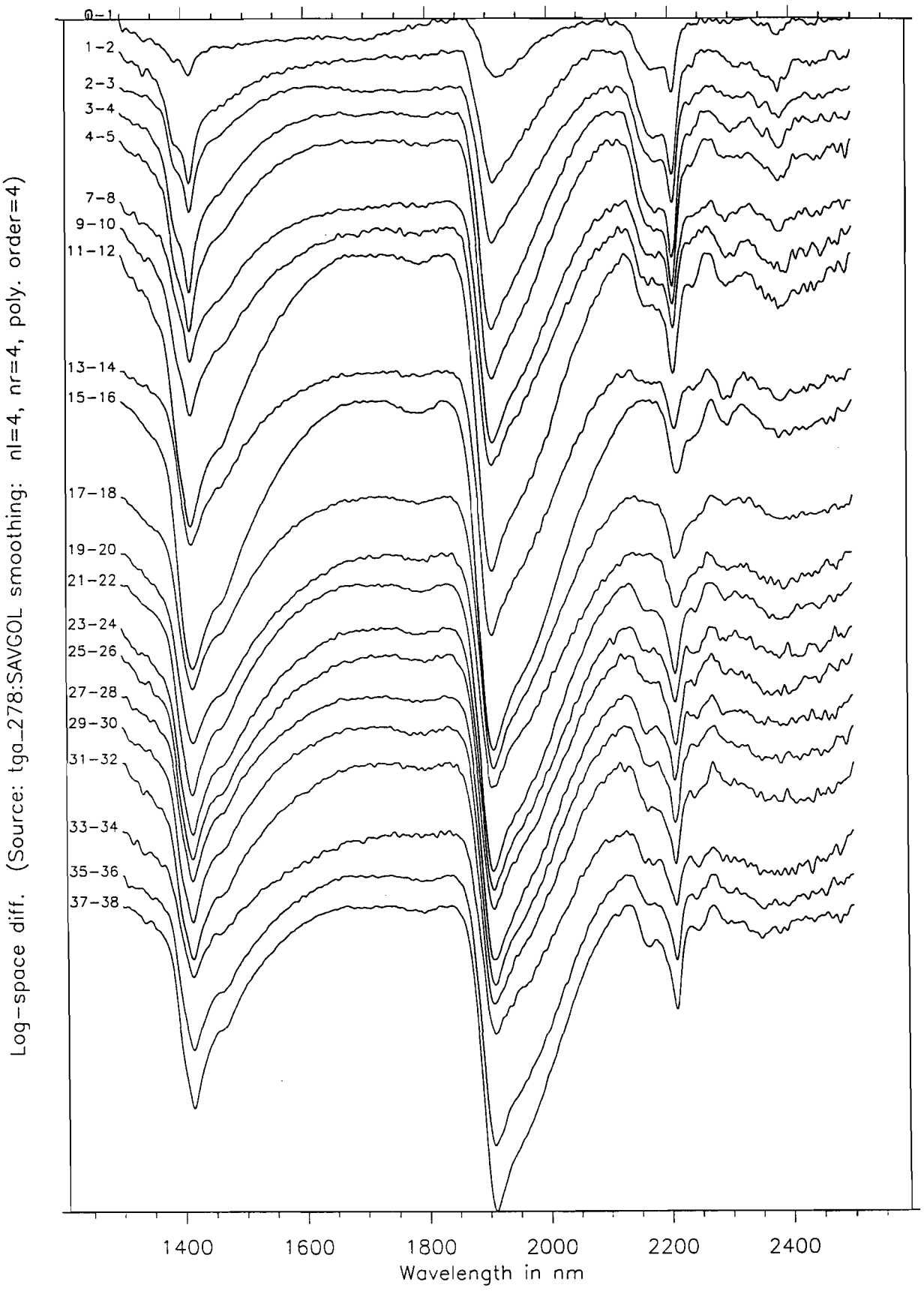

drill hole tga 278

Table A-2 Salient Spectral Features Drill Hole TGA 282

0 - 2 m	K1 kaolinite
2 - 4 m	mixture of K1 and K2 kaolinite responses
4 - 14 m	K2 kaolinite responses
15 - 16 m	strong montmorillonite and weak K2 kaolinite responses
17 - 54 m	strong montmorillonite response
55 - 60 m	weaker montmorillonite response and weak chlorite response (less-weathered basement ?)

The Fe-OH-Al substitution feature at 2239nm is evident from the surface down to 16m, which corresponds to the kaolinite distribution.
The 2295nm absorption feature, which is considered to indicate Fe-rich smectite, extends from 11 to 18m.

Stacked Spectral Profile **TGA 282**

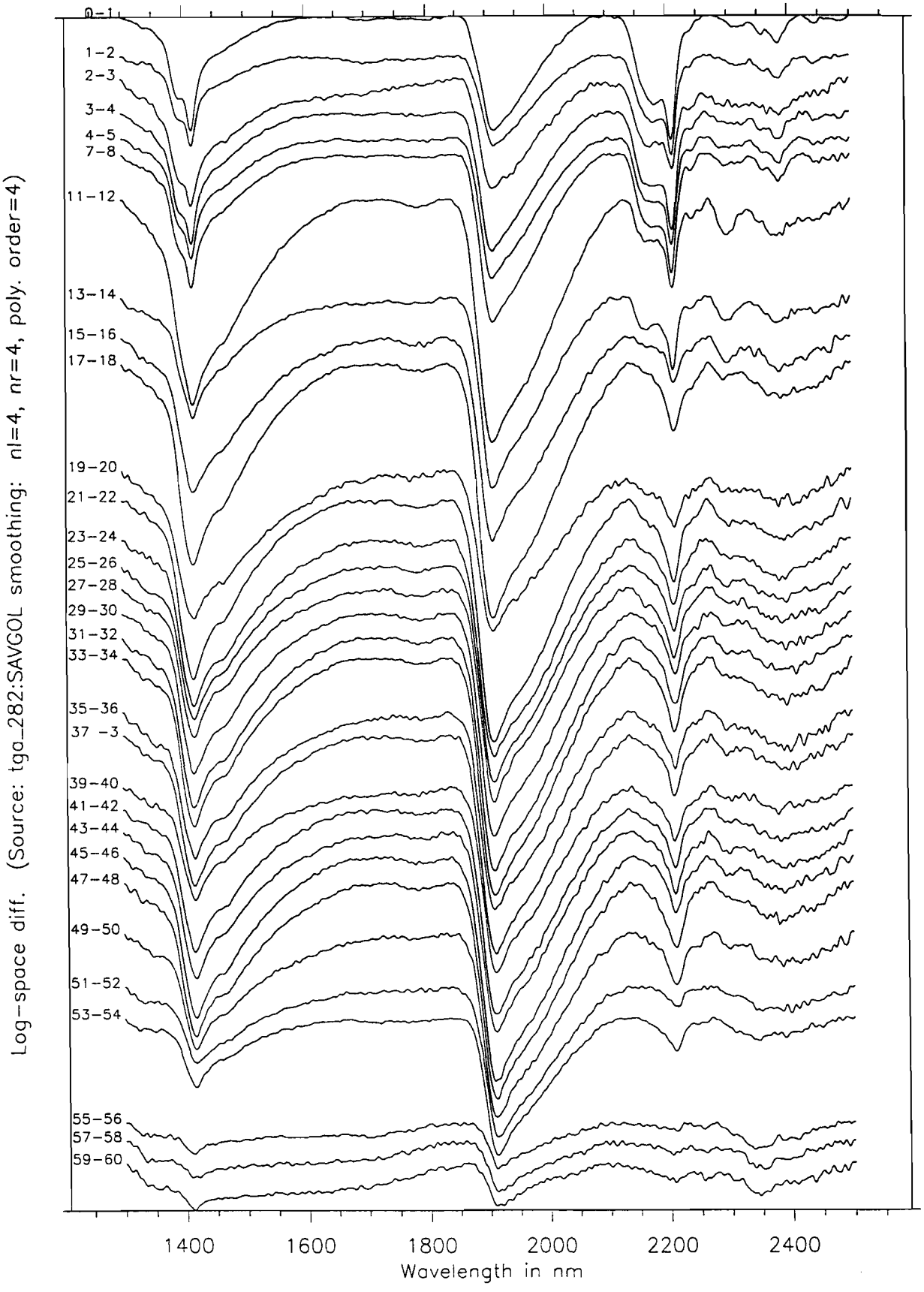

Drill Hole tga 282

I-4

Table A-3 Salient Spectral Features Drill Hole TGA 283

0 - 5 m	K1 kaolinite
7 - 14 m	K2 kaolinite responses
15 - 16 m	K2 kaolinite responses and montmorillonite
17 - 22 m	strong montmorillonite response

The Fe-OH-Al substitution feature at 2239nm extends from the surface down to 22m. The 2295nm Fe-rich smectite feature is strong from 9 to 16m, and an absorption doublet, possibly related to this feature, results in features at 2286 and 2303 nm from 17 to 22m

Stacked Spectral Profile **TGA 283**

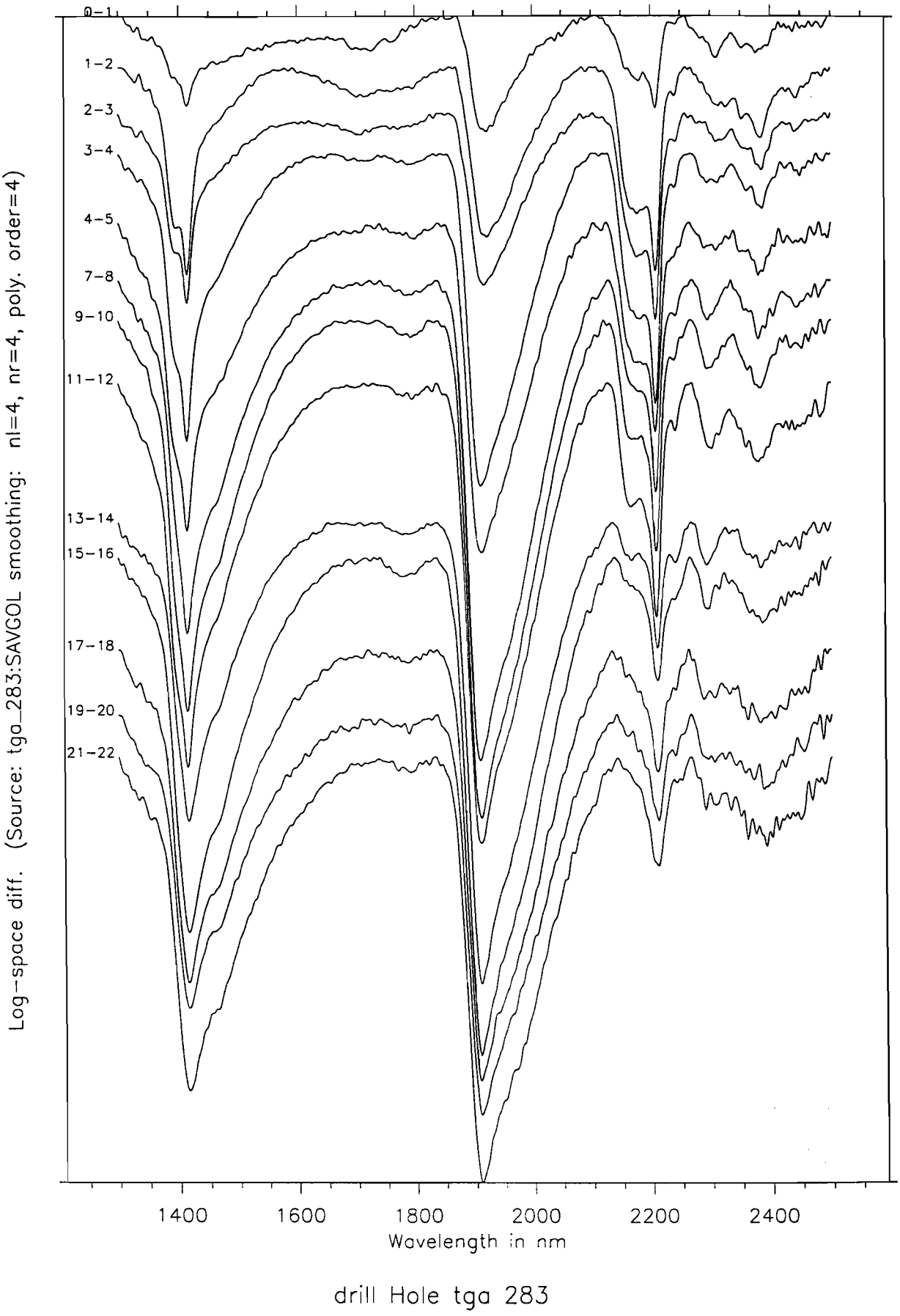

drill Hole tga 283

Table A-4 Salient Spectral Features Drill Hole TGA 285

0 - 8 m	K1 kaolinite
9 - 10 m	mixture of K1 and K2 kaolinite responses
11 - 20 m	K2 kaolinite responses
21 - 24 m	K2 kaolinite responses & montmorillonite
25 - 31 m	strong montmorillonite response

The Fe-OH-Al substitution feature at 2239nm extends from the surface down to 22m.
The 2295nm Fe-rich smectite feature is strong from 9 to 26m.

Stacked Spectral Profile **TGA 285**

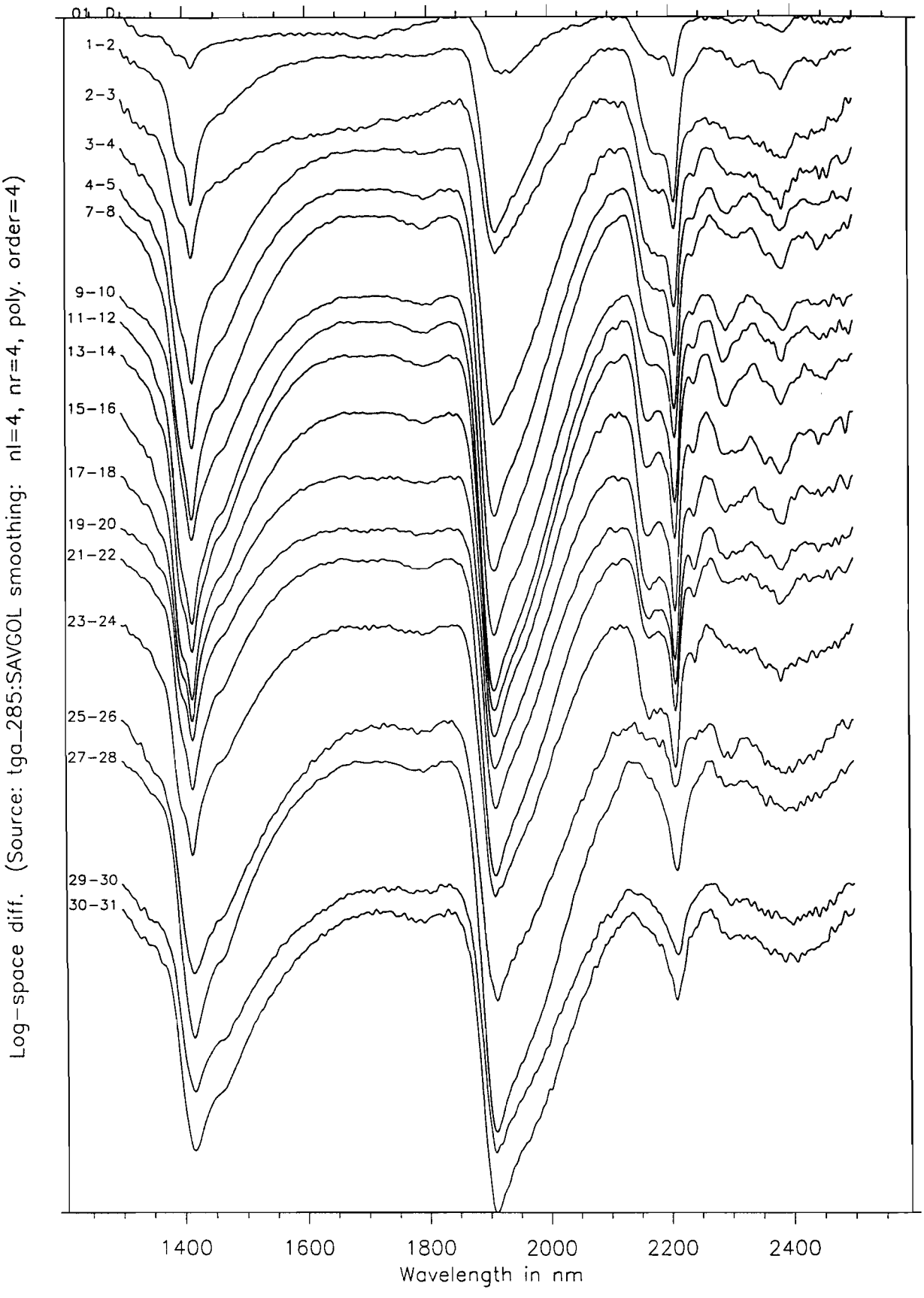

drill hole tga 285

I-8

Table A-5 Salient Spectral Features Drill Hole TGA 295

0 - 8 m	K1 kaolinite
9 - 10 m	mixture of K1 kaolinite and montmorillonite responses
11 - 14 m	mixture of K2 kaolinite and montmorillonite responses
15 - 24 m	strong montmorillonite response

The Fe-OH-Al substitution feature at 2239nm extends from the surface down to 16m with related (?) weaker absorptions to 24m.
The 2295nm Fe-rich smectite feature is strong from 9 to 24m.

Stacked Spectral Profile **TGA 295**

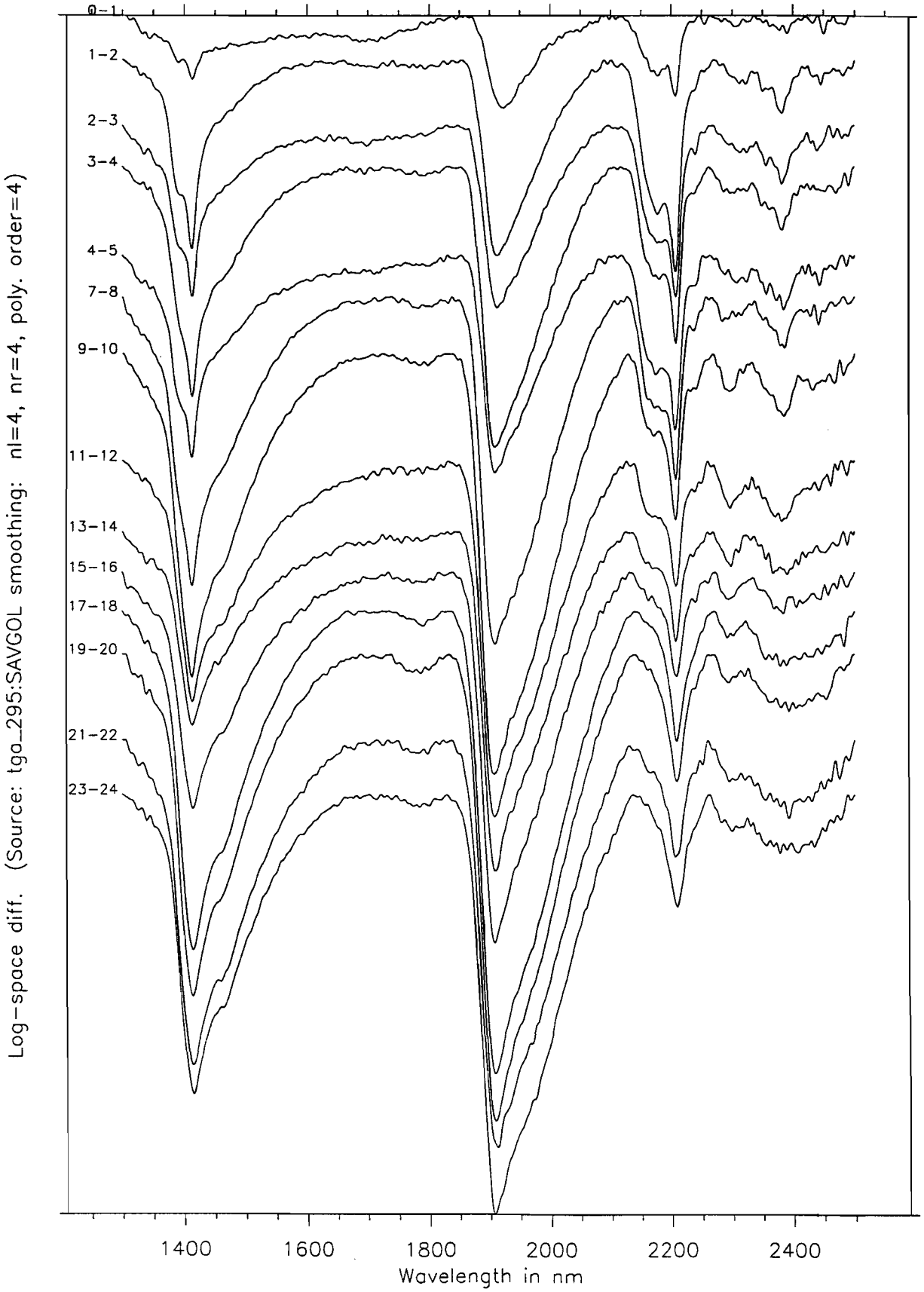

drill hole tga 295

Table A-6 Salient Spectral Features Drill Hole TGA 300

0 - 3 m	K1 kaolinite
3 - 8 m	mixture of K1 & K2 kaolinite responses
8 - 18 m	K2 kaolinite
15 - 24 m	strong montmorillonite and weaker K2 kaolinite responses
25 - 33m	strong montmorillonite

The Fe-OH-Al substitution feature at 2239nm extends from the surface down to 26m. The 2295nm Fe-rich smectite feature is strong from 7 to 10m and from 17 to 20 m. Weaker absorptions occur from 3 to 5m, and from 21 to 33m. The depth interval from 11 to 16m contains broader absorption features, which may or may not be related to Fe-rich smectite.

Stacked Spectral Profile **TGA 300**

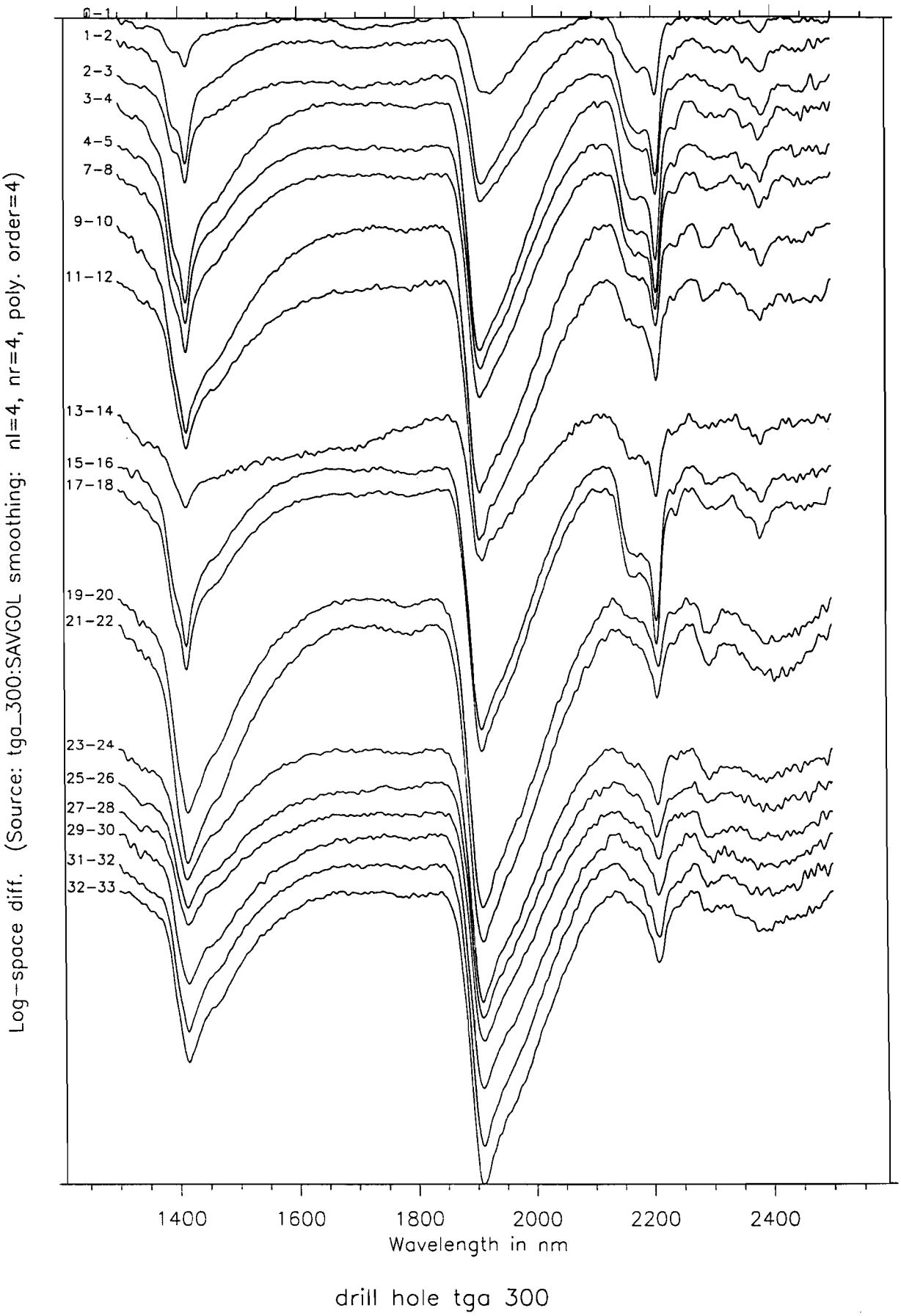

drill hole tga 300

Table A-7 Salient Spectral Features Drill Hole TGA 306

0 - 16 m	K1 kaolinite
17 - 18 m	?? (dolomite ?)
19 - 30 m	K2 kaolinite

The Fe-OH-Al substitution feature at 2239nm extends from the surface down to 30m.
The 2295nm Fe-rich smectite feature is strong from 7 to 12m.

Stacked Spectral Profile **TGA 306**

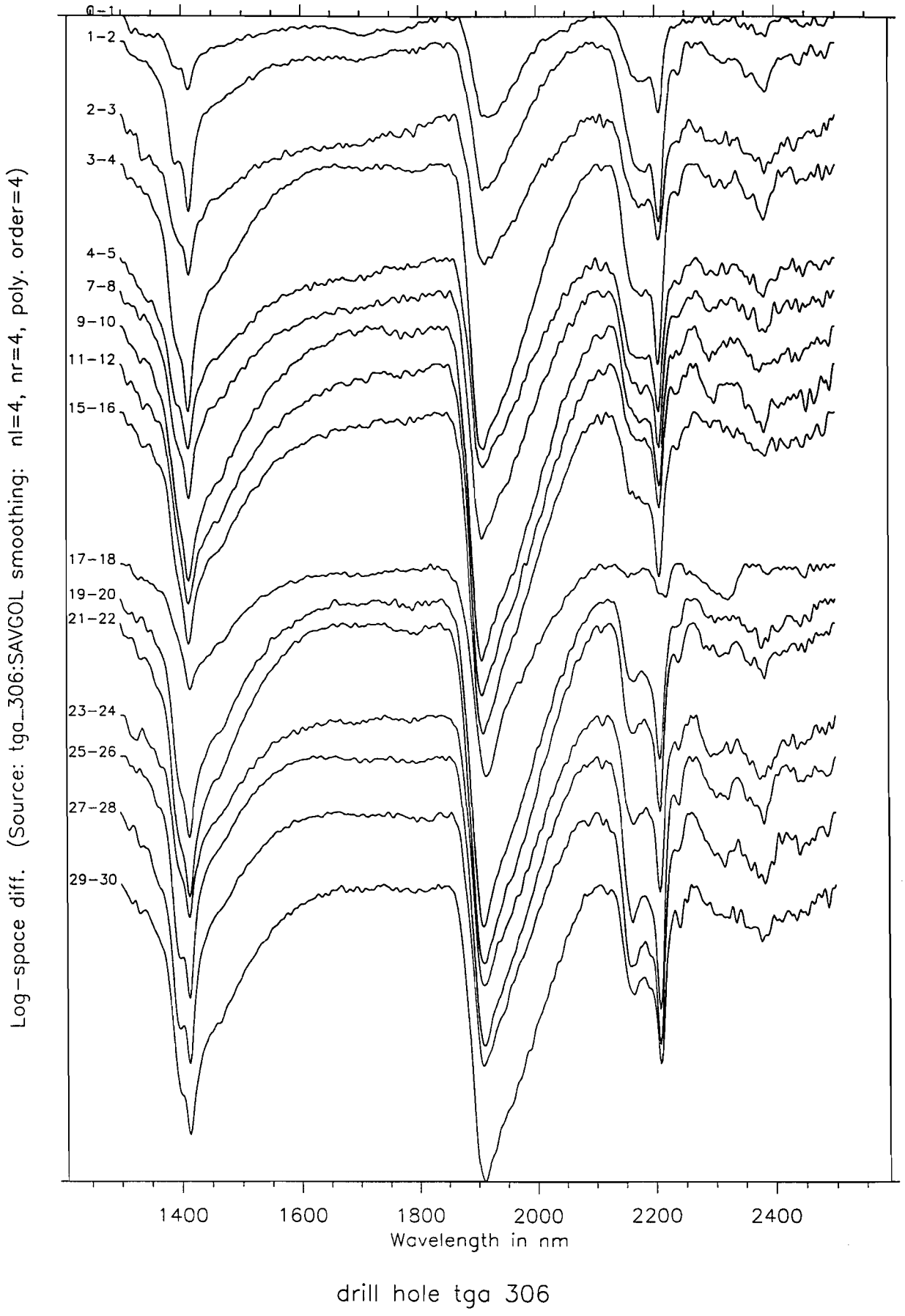

Table A-8 Salient Spectral Features Drill Hole TGA 364

0 - 10 m	K1 kaolinite
11 - 14 m	mixture of K1 kaolinite & montmorillonite responses
15 - 16 m	mixture of K1 & K2 kaolinite & montmorillonite responses
17 - 18 m	K2 kaolinite & weaker montmorillonite responses
19 - 28 m	K2 kaolinite

The Fe-OH-Al substitution feature at 2239nm extends from the surface down to 28m. The 2295nm Fe-rich smectite feature is strong from 9 to 20m. The depth interval from 21 to 28m contains a broader absorption feature, which may or may not be related to Fe-rich smectite.

Stacked Spectral Profile **TGA 364**

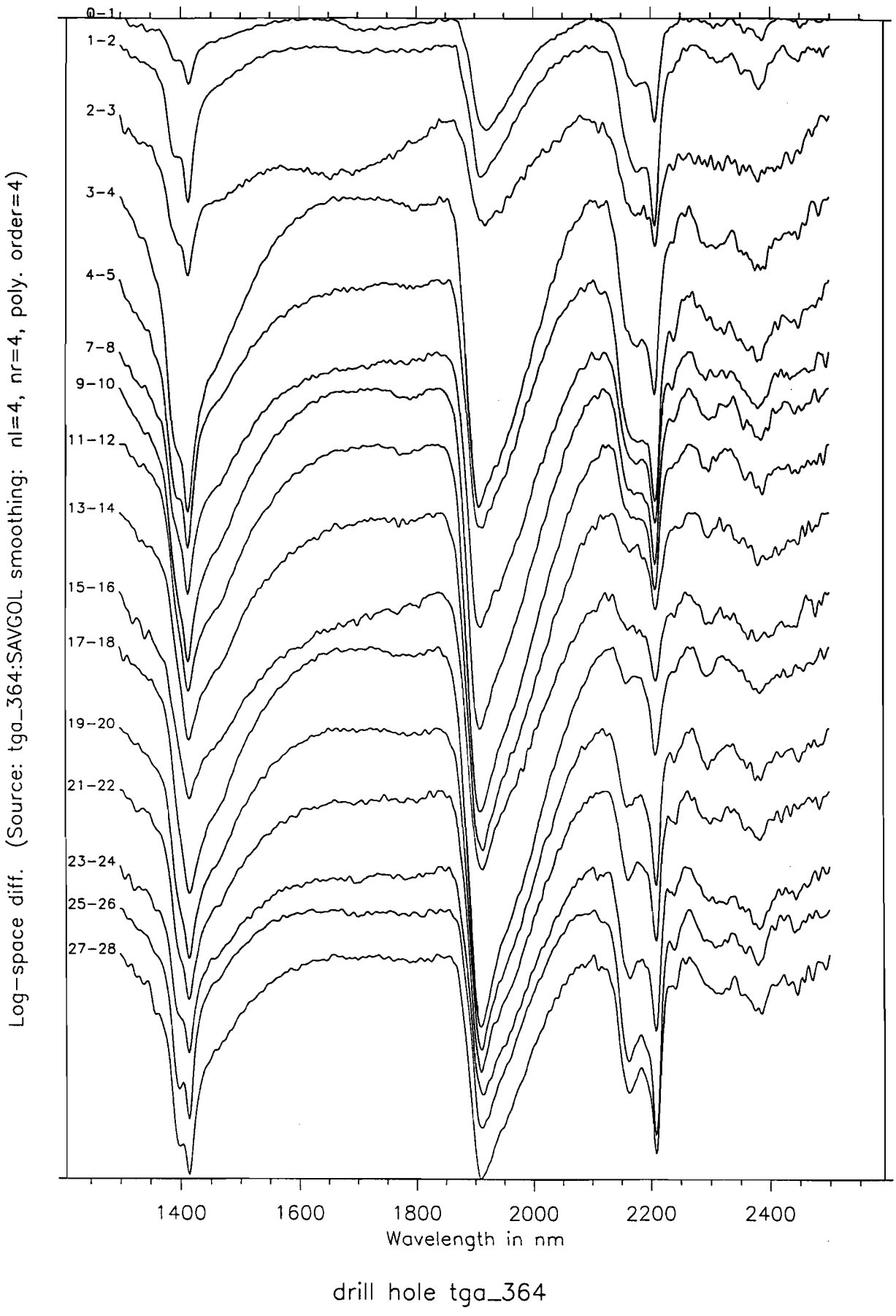

drill hole tga_364

APPENDIX II : GEOCHEMICAL ASSAYS DRILLHOLE TGA 278

Sample No	134893	134894	134895	134896	134897	134898	134899	134900	134901	134902
Depth (m)	0-1	1- 2	2-3	3-4	4-5	7-8	9-10	11-12	13-14	15-16
Fe (%)	1.07	1.79	18.10	6.99	5.54	4.86	6.65	5.27	8.89	5.20
Mn (ppm)	107	119	159	122	203	1850	1260	383	1650	1700
Na (%)	0.045	0.043	0.038	0.080	0.127	0.133	0.237	0.302	0.485	0.366
K (%)	0.15	0.18	0.14	0.15	0.26	-0.10	-0.10	-0.10	0.17	0.12
As (ppm)	1.31	2.22	31.00	10.90	5.63	3.40	3.47	1.44	2.28	0.83
Au (ppb)	2.0	4.1	-2.0	2.9	-2.0	-2.0	12.8	32.6	-2.0	6.4
Ba (ppm)	73.7	66.4	77.9	219.0	162.0	507.0	344.0	-50.0	415.0	447.0
Br (ppm)	1.06	2.28	-0.50	1.01	2.09	-0.50	2.10	1.95	-0.50	0.77
Ce (ppm)	24.30	26.40	39.60	17.20	24.50	313.00	38.00	27.40	31.40	13.30
Co (ppm)	6.07	6.54	26.40	11.30	9.28	138.00	37.80	15.40	37.90	30.70
Cr (ppm)	30.1	46.9	181.0	63.5	53.3	41.8	53.6	44.8	64.2	73.0
Cs (ppm)	1.41	2.63	2.52	2.03	2.51	1.47	1.76	2.08	1.28	1.03
Cu (ppm)	15	20	64	34	30	53	47	54	80	31
Eu (ppm)	-0.50	0.55	1.14	-0.50	-0.50	3.34	2.26	1.73	1.09	0.91
Hf (ppm)	7.36	8.07	7.80	6.36	6.14	5.17	3.16	1.65	1.70	0.71
La (ppm)	10.50	11.00	16.90	11.40	13.00	66.90	65.50	37.70	13.80	15.10
Lu (ppm)	0.20	0.26	0.49	0.23	0.20	0.82	0.46	0.47	0.22	0.25
Pb (ppm)	10	11	46	26	22	17	10	-5	-5	6
Rb (ppm)	16.5	28.4	33.5	19.1	32.5	-10.0	18.5	17.4	28.2	26.2
Sb (ppm)	0.14	0.24	0.91	0.45	0.28	0.15	0.19	0.20	-0.10	-0.10
Sc (ppm)	5.28	9.75	25.90	13.70	15.10	18.80	21.80	26.80	30.20	17.40
Sm (ppm)	2.07	2.29	5.26	2.26	1.89	13.90	9.46	6.81	3.56	3.12
Ta (ppm)	-1.00	-1.00	1.26	-1.00	1.12	1.29	-1.00	-1.00	1.07	-1.00
Th (ppm)	5.29	7.00	17.40	10.90	9.39	8.75	6.85	5.21	3.11	1.68
U (ppm)	-1.00	1.26	5.62	1.61	1.11	1.19	-1.00	-1.00	-1.00	-1.00
W (ppm)	4.98	3.04	-1.00	1.78	2.23	-1.00	-1.00	-1.00	-1.00	-1.00
Yb (ppm)	1.51	1.78	3.70	1.85	1.64	6.38	3.43	3.55	1.84	1.82
Zn (ppm)	22.0	25.0	26.0	23.0	33.0	85.0	64.0	60.0	58.0	65.0

APPENDIX III : GEOCHEMICAL ASSAYS DRILLHOLE TGA 282

Sample No	134813	134814	134815	134816	134817	134818	134819	134820	134821	134822	134823	134824	134825	134826	134827	134828
Depth (m)	0-1	1-2	2-3	3-4	4-5	7-8	11-12	13-14	15-16	17-18	19-20	21-22	23-24	25-26	27-28	29-30
Fe (%)	5.48	12.90	10.60	9.38	6.19	4.48	5.02	10.60	5.41	5.30	4.84	4.96	5.57	6.77	5.65	6.23
Mn (ppm)	175	185	118	108	140	146	595	2660	591	258	362	454	800	1480	1530	1180
Na (%)	0.047	0.036	0.078	0.084	0.080	0.108	0.227	0.289	0.658	0.945	0.444	0.358	0.267	0.329	0.491	0.309
K (%)	0.14	0.12	0.22	0.25	0.28	0.50	0.14	-0.10	0.45	0.92	1.12	1.31	1.21	1.23	1.13	1.17
As (ppm)	7.19	18.70	10.90	8.23	5.62	4.15	0.67	4.24	1.75	2.11	1.75	1.08	1.63	1.89	1.64	1.84
Au (ppb)	6.3	-2.0	-2.0	-2.0	-2.0	2.4	-2.0	4.7	3.4	-2.0	8.6	11.8	4.0	9.9	5.7	4.9
Ba (ppm)	56.5	58.3	230.0	307.0	811.0	296.0	1040.0	708.0	1170.0	439.0	582.	723.0	644.0	766.0	888.0	568.0
Br (ppm)	2.61	1.23	1.04	1.37	1.32	1.77	1.97	1.07	0.69	0.80	0.57	-0.50	0.84	0.78	0.57	-0.50
Ce (ppm)	31.50	53.60	17.30	12.70	16.10	22.00	30.40	41.60	76.70	60.90	68.50	76.80	82.00	96.10	84.40	78.60
Co (ppm)	15.20	20.80	7.90	6.26	6.78	8.36	23.30	48.40	13.60	10.70	18.70	12.00	15.30	25.00	30.70	24.30
Cr (ppm)	85.2	150.0	69.9	58.7	52.0	46.2	42.3	53.7	39.5	22.8	28.0	22.8	27.2	28.1	25.1	26.3
Cs (ppm)	3.65	2.78	3.03	2.56	3.07	3.29	1.43	1.36	1.14	1.30	1.77	2.03	2.49	2.91	1.38	2.94
Cu (ppm)	34	53	39	32	30	29	33	46	30	42	53	45	92	67	97	58
Eu (ppm)	0.63	0.84	-0.50	-0.50	-0.50	-0.50	1.29	1.19	2.05	1.48	1.49	1.49	1.87	2.02	1.90	1.59
Hf (ppm)	7.69	6.87	5.01	5.30	7.11	6.65	2.25	4.68	3.75	4.16	4.55	4.50	4.59	6.19	4.63	4.74
La (ppm)	11.10	12.60	11.70	10.20	9.79	15.90	24.50	24.00	43.30	35.60	32.70	35.70	36.80	47.70	50.70	36.90
Lu (ppm)	0.33	0.35	-0.20	-0.20	-0.20	-0.20	0.34	0.23	0.62	0.25	0.42	0.26	0.53	0.40	0.34	0.29
Pb (ppm)	18	35	30	21	19	19	6	8	9	10	9	14	13	9	8	9
Rb (ppm)	33.8	32.0	27.9	35.2	42.9	49.7	34.1	20.6	29.5	55.6	57.5	62.4	67.3	75.5	60.5	63.5
Sb (ppm)	0.41	0.67	0.36	0.27	0.31	0.28	0.10	0.20	0.11	-0.10	-0.10	-0.10	-0.10	-0.10	-0.10	-0.10
Sc (ppm)	15.70	21.20	18.40	16.50	16.00	16.30	21.00	19.90	19.40	24.70	24.30	22.80	27.00	32.60	25.70	28.70
Sm (ppm)	3.01	3.66	1.97	1.41	1.59	2.04	5.26	4.63	8.15	6.92	6.15	6.63	8.39	9.25	8.10	7.18
Ta (ppm)	-1.00	-1.00	-1.00	1.10	-1.00	1.32	1.27	1.11	1.59	-1.00	-1.00	1.09	1.32	1.27	1.40	1.53
Th (ppm)	9.88	15.00	14.90	14.00	11.80	10.40	6.52	4.85	5.32	6.17	6.45	6.63	4.72	6.36	7.96	5.90
U (ppm)	2.99	4.32	1.96	1.20	1.05	1.35	1.13	1.43	-1.00	-1.00	-1.00	-1.00	-1.00	-1.00	-1.00	-1.00
W (ppm)	2.96	1.17	1.68	1.27	2.12	3.23	1.37	3.25	1.85	2.00	-1.00	-1.00	2.75	-1.00	-1.00	-1.00
Yb (ppm)	2.29	2.80	1.51	1.19	1.52	1.56	2.63	1.91	4.75	2.23	3.16	2.06	4.02	3.14	2.83	2.21
Zn (ppm)	26.0	28.0	36.0	36.0	35.0	35.0	61.0	62.0	51.0	68.0	78.0	81.0	98.0	104.0	98.0	99.0

APPENDIX IV : GEOCHEMICAL ASSAYS DRILLHOLE TGA 295

Sample No	134943	134944	134945	134946	134947	134948	134949	134950	134951	134952	134953	134954
Depth (m)	0-1	1-2	2-3	3-4	4-5	7-8	9-10	11-12	13-14	15-16	17-18	19-20
Fe (%)	0.46	6.44	8.11	4.46	5.07	3.99	3.54	4.06	4.71	3.67	3.73	4.00
Mn (ppm)	103	202	260	142	159	87	311	1020	5000	2360	940	408
Na (%)	0.014	0.149	0.164	0.133	0.153	0.164	0.181	0.131	0.242	0.585	0.892	0.619
K (%)	-0.10	0.33	0.35	0.35	0.38	0.41	0.57	-0.10	-0.10	0.29	0.87	0.97
As (ppm)	0.65	8.04	8.42	3.08	4.57	1.73	0.67	2.44	1.30	0.58	1.29	1.85
Au (ppb)	-2.0	4.8	-2.0	-2.0	-2.0	-2.0	-2.0	-2.0	7.1	27.0	42.7	-2.0
Ba (ppm)	-50.0	142.0	147.0	2080.0	299.0	305.0	479.0	294.0	1310.0	835.0	575.0	536.0
Br (ppm)	0.90	2.09	1.07	1.29	1.39	2.57	0.85	0.55	-0.50	-0.50	-0.50	-0.50
Ce (ppm)	16.10	38.60	138.00	18.50	20.90	16.70	91.90	55.80	67.90	33.00	59.80	53.70
Co (ppm)	4.93	15.90	21.60	11.80	8.51	9.12	14.50	41.50	83.80	34.20	16.10	12.50
Cr (ppm)	24.4	91.6	64.7	46.6	42.7	36.6	35.3	29.9	30.2	24.8	20.5	17.6
Cs (ppm)	0.78	4.62	3.45	2.88	2.94	3.54	2.93	0.81	1.79	1.65	1.91	1.21
Cu (ppm)	8	35	42	28	25	28	28	39	43	32	34	36
Eu (ppm)	-0.50	0.96	0.73	-0.50	-0.50	-0.50	1.44	1.44	1.53	1.06	1.36	1.43
Hf (ppm)	7.06	8.35	7.03	5.71	6.80	2.57	3.62	4.12	3.24	2.51	2.94	3.31
La (ppm)	8.61	18.90	16.00	13.80	13.50	15.60	34.30	30.60	27.50	16.80	31.60	41.90
Lu (ppm)	-0.20	0.41	0.33	0.21	0.23	-0.20	0.36	0.32	0.44	0.28	0.22	0.24
Pb (ppm)	6	17	32	10	10	13	8	13	13	8	11	10
Rb (ppm)	12.8	51.3	33.0	36.2	36.9	49.2	65.9	10.7	23.7	27.4	52.9	45.4
Sb (ppm)	0.13	0.39	0.45	0.16	0.27	0.18	0.21	0.17	-0.10	-0.10	-0.10	-0.10
Sc (ppm)	2.97	18.60	17.40	17.60	13.70	18.40	15.10	17.50	21.50	19.80	18.00	23.10
Sm (ppm)	1.60	4.16	3.31	1.94	1.93	1.73	5.71	5.94	5.43	3.51	5.66	5.97
Ta (ppm)	-1.00	-1.00	1.15	1.02	-1.00	1.28	-1.00	-1.00	-1.00	1.50	1.16	1.04
Th (ppm)	4.27	12.10	12.00	9.40	9.39	8.72	9.01	6.78	8.07	6.23	5.76	6.63
U (ppm)	-1.00	2.82	2.22	-1.00	-1.00	-1.00	1.66	-1.00	1.61	1.67	-1.00	-1.00
W (ppm)	1.13	-1.00	1.38	1.62	1.19	-1.00	1.31	1.81	2.42	3.38	1.80	1.74
Yb (ppm)	1.24	2.71	2.35	1.50	1.59	0.93	2.63	2.30	3.10	2.00	1.67	1.86
Zn (ppm)	9.0	32.0	34.0	43.0	36.0	58.0	62.0	57.0	65.0	54.0	58.0	56.0

APPENDIX V : GEOCHEMICAL ASSAYS DRILLHOLE TGA 300

Sample No	134957	134958	134959	134960	134961	134962	134963	134964	134965	134966	134967	134968
Depth (m)	0-1	1-2	2-3	3-4	4-5	7-8	9-10	11-12	13-14	15-16	17-18	19-20
Fe (%)	0.76	15.80	13.20	5.52	5.47	6.76	3.72	2.65	3.65	5.02	5.27	4.66
Mn (ppm)	238	318	2160	259	165	190	900	1350	3790	668	542	400
Na (%)	0.021	0.124	0.065	0.137	0.131	0.114	0.155	0.167	0.129	0.151	0.086	0.652
K (%)	0.16	0.31	0.25	0.54	0.43	0.47	0.67	0.74	0.57	0.42	-0.10	1.34
As (ppm)	0.70	22.10	14.70	3.02	2.78	8.77	1.09	1.57	3.08	1.88	1.84	1.30
Au (ppb)	-2.0	-2.0	-2.0	-2.0	-2.0	-2.0	3.7	3.2	-2.0	4.6	-2.0	5.2
Ba (ppm)	72.2	160.0	532.0	324.0	802.0	223.0	491.0	599.0	945.0	1140.0	97.3	831.0
Br (ppm)	1.63	1.20	0.78	0.70	1.67	1.78	2.46	1.52	0.67	0.87	0.71	-0.50
Ce (ppm)	21.30	54.40	288.00	21.50	18.50	20.80	80.80	68.80	82.70	54.60	35.90	60.00
Co (ppm)	4.84	18.50	30.20	11.10	10.10	10.20	21.30	17.50	46.50	16.80	18.60	13.60
Cr (ppm)	26.3	165.0	98.6	34.0	39.5	52.1	32.0	27.3	30.0	43.2	41.6	25.2
Cs (ppm)	1.33	2.91	2.19	4.63	4.63	3.74	3.20	2.45	2.14	2.34	1.26	3.81
Cu (ppm)	13	58	55	36	31	37	28	23	30	38	38	38
Eu (ppm)	-0.50	1.23	0.85	-0.50	-0.50	-0.50	0.69	1.25	2.14	1.67	1.22	1.40
Hf (ppm)	9.24	6.75	7.22	4.45	4.25	5.10	2.69	4.16	5.22	5.79	5.70	4.30
La (ppm)	10.20	19.40	17.90	13.40	13.10	15.10	23.50	34.80	55.20	37.10	23.80	31.70
Lu (ppm)	0.23	0.43	0.36	-0.20	-0.20	0.21	0.26	0.41	0.44	0.37	0.35	0.47
Pb (ppm)	5	28	68	18	9	28	12	19	23	12	7	12
Rb (ppm)	17.0	43.2	29.7	65.4	54.4	54.6	73.0	68.1	45.6	28.9	12.1	52.1
Sb (ppm)	0.14	0.85	0.65	0.29	0.25	0.24	0.13	0.14	0.14	0.20	0.20	-0.10
Sc (ppm)	4.58	26.60	18.60	20.90	20.80	14.20	11.40	11.30	15.60	24.60	27.10	22.30
Sm (ppm)	1.91	4.77	4.33	2.05	1.90	2.30	3.81	6.06	9.66	7.68	5.07	5.89
Ta (ppm)	-1.00	1.18	-1.00	-1.00	-1.00	-1.00	-1.00	-1.00	-1.00	1.21	-1.00	1.22
Th (ppm)	5.82	18.10	13.30	11.80	11.80	10.10	7.06	9.10	10.80	11.40	9.56	6.59
U (ppm)	1.14	4.70	3.40	-1.00	-1.00	1.32	1.17	1.14	1.72	1.30	-1.00	-1.00
W (ppm)	2.03	-1.00	-1.00	1.15	1.13	1.12	-1.00	2.30	2.14	1.55	1.37	1.52
Yb (ppm)	1.56	3.10	2.80	1.47	1.38	1.62	1.97	2.85	3.14	2.81	2.67	3.40
Zn (ppm)	18.0	37.0	37.0	60.0	57.0	40.0	58.0	49.0	58.0	80.0	90.0	68.0